AD-A185 568 THE PRODUCTION OF TURBULENCE IN BOUNDARY LAYERS -- THE ROLE OF MICROSCALE..(U) MICHIGAN STATE UNIV EAST LANSING TURBULENCE STRUCTURE LAB R E FALCO JUN 87 1/2

UNCLASSIFIED TSL-87-3 AFOSR-TR-87-1194 F49620-85-C-0002 F/G 20/4 NL

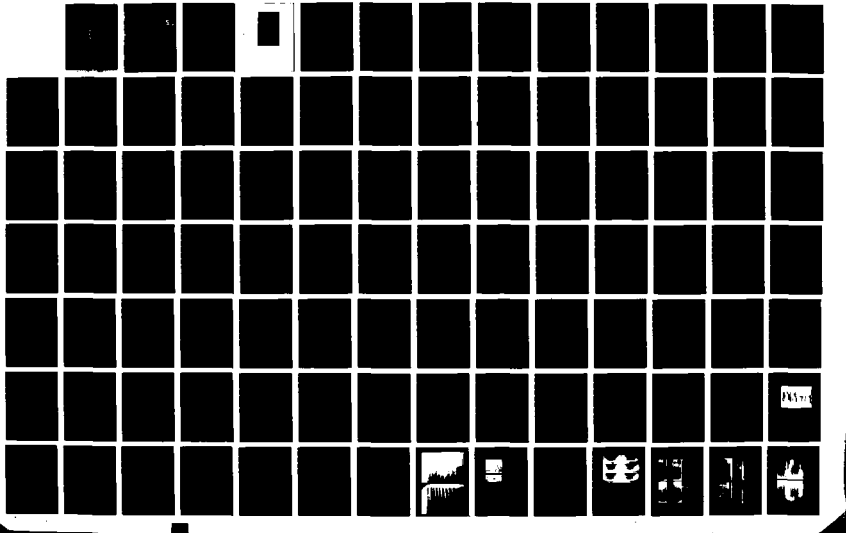

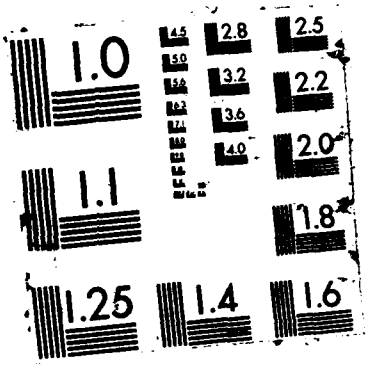
1.0
1.1
1.25
1.4
1.6
1.8
2.0
2.2
2.5
2.8
3.2
3.6
4.0
4.5
5.0

(2)

AD-A185 568

REPORT DOCUMENTATION PAGE

1b. RESTRICTIVE MARKINGS: DTIC FILE COPY

2a. SECURITY CLASSIFICATION AUTHORITY

2b. DECLASSIFICATION / DOWNGRADING SCHEDULE

3. DISTRIBUTION / AVAILABILITY OF REPORT: Unlimited

4. PERFORMING ORGANIZATION REPORT NUMBER(S)

5. MONITORING ORGANIZATION REPORT NUMBER(S): AFOSR-TR- 87-1194

6a. NAME OF PERFORMING ORGANIZATION: Michigan State University

6b. OFFICE SYMBOL (If applicable)

7a. NAME OF MONITORING ORGANIZATION: AFOSR

6c. ADDRESS (City, State, and ZIP Code): East Lansing, MI 48824

7b. ADDRESS (City, State, and ZIP Code): AFOSR/NA, Bldg 410, Bolling Air Force Base, Washington, DC

DTIC ELECTE OCT 07 1987

8a. NAME OF FUNDING / SPONSORING ORGANIZATION: AF OFFICE OF SCIENTIFIC RESEARCH

8b. OFFICE SYMBOL (If applicable): AFOSR/NA

9. PROCUREMENT INSTRUMENT IDENTIFICATION NUMBER: ~~AFOSR Contract No.~~ F49620-85-C-0002

8c. ADDRESS (City, State, and ZIP Code): AFOSR/NA, Bldg 410, Bolling AFB, DC 20332

10. SOURCE OF FUNDING NUMBERS

PROGRAM ELEMENT NO.	PROJECT NO.	TASK NO.	WORK UNIT ACCESSION NO.
61102F	2307	A2	

11. TITLE (Include Security Classification): The Production of Turbulence in Boundary Layers -- The Role of Microscale Coherent Motions

12. PERSONAL AUTHOR(S): R. E. Falco

13a. TYPE OF REPORT	13b. TIME COVERED	14. DATE OF REPORT (Year, Month, Day)	15. PAGE COUNT
Final	FROM 10/1/84 TO 9/30/86	June 1987	104

16. SUPPLEMENTARY NOTATION

17. COSATI CODES			18. SUBJECT TERMS (Continue on reverse if necessary and identify by block number)
FIELD	GROUP	SUB-GROUP	TURBULENCE, BOUNDARY LAYER

19. ABSTRACT (Continue on reverse if necessary and identify by block number)

We have further explored the details of the turbulence production process in turbulent boundary layers. Additional details of the process in the wall region have been clarified, especially the formation of the long streaky structure, and secondary hairpin vorticity. It appears that the outer region microscale coherent motion called a Typical eddy plays a dominant role in the process. Long time averaged statistics of the two-point vorticity-vorticity correlations have been obtained which support the conditionally sampled data and interpretations. The Typical eddy produces the long streaks along with the pockets, and one of the hairpins directly. Several other hairpins form from the evolution of the vorticity produced by the passage of the typical eddy over the wall. A model of the typical eddy/wall region interaction, i.e., a vortex ring/Stokes layer interaction, was investigated to see if it could reproduce all of the morphology. It was

(Continued on other side)

20. DISTRIBUTION / AVAILABILITY OF ABSTRACT: ☒ UNCLASSIFIED/UNLIMITED ☐ SAME AS RPT. ☐ DTIC USERS

21. ABSTRACT SECURITY CLASSIFICATION: UNCLASSIFIED

22a. NAME OF RESPONSIBLE INDIVIDUAL: Dr. Jim McMichael

22b. TELEPHONE (Include Area Code): (202) 767-4935

22c. OFFICE SYMBOL: AFOSR/NA

DD FORM 1473, 84 MAR — 83 APR edition may be used until exhausted. All other editions are obsolete.

SECURITY CLASSIFICATION OF THIS PAGE

19. ABSTRACT (Cont.)

found that the model can produce all of the turbulent boundary layer features associated with production, including the long streaks. Using the model we have gained new insights into the sensitivity of the production process. It has also been found that relatively small differences in the convection velocity of the excitation eddies result in the difference between turbulent boundary layer production and spot production (which involves very strong lateral production). Our data suggest that there are many combinations of parameters that can result in critical conditions. Considerable work remains to understand the role played by these variables. This understanding will hopefully lead to development of ideas of self-similarities in the process, such that the production of turbulence may be more simply understood, and more easily controlled.

THE PRODUCTION OF TURBULENCE IN BOUNDARY LAYERS: THE ROLE OF MICROSCALE COHERENT MOTIONS

R. E. Falco

Final Report

Prepared from work done under

AFOSR Contract F49620-85-C-0002

Report TSL-87-3

Turbulence Structure Laboratory

Department of Mechanical Engineering

Michigan State University

East Lansing, MI 48824

1. ABSTRACT

We have further explored the details of the turbulence production process in turbulent boundary layers. Additional details of the process in the wall region have been clarified, especially the formation of the long streaky structure, and secondary hairpin vorticity. It appears that the outer region microscale coherent motion called a Typical eddy plays the dominant role in the process. Long time averaged statistics of the two-point vorticity-vorticity correlations ~~have been obtained which~~ support the conditionally sampled data and interpretations. The Typical eddy produces the long streaks along with the pockets, and one of the hairpins directly. Several other hairpins form from the evolution of the vorticity produced by the passage of the typical eddy over the wall. A model of the Typical eddy/wall region interaction, i.e., a vortex ring/Stokes layer interaction, was investigated to see if it could reproduce all of the morphology. It was found that the model can produce all of the turbulent boundary layer features associated with production, including the long streaks. By using the model, we have gained new insights into the sensitivity of the production process. ~~It has also been found that~~ relatively small differences in the convection velocity of the excitation eddies have been found to result in the difference between turbulent boundary layer production and spot production (which involves very strong lateral production). Our data suggest that there are many combinations of parameters that can result in critical conditions. Considerable work remains to understand the role played by these variables. This understanding will hopefully lead to development of ideas of self-

similarities in the process, such that the production of turbulence may be more simply understood, and more easily controlled.

2. GENERAL INTRODUCTION

Over the past year we have discovered the mechanism of production of the long streaks, and a mechanism for creation of the vortex ring-like Typical eddies, and demonstrated the occurrence of both within a real turbulent boundary layer. These aspects were the missing links needed to complete the conceptual structural model. This model puts the formation of hairpin vortices into the perspective of being a part of a multifaceted bursting process, rather than the cause of the bursting process. However, experimental determination of the relative importance of each of the elements of the model in low Reynolds number layers is far from complete, and we know very little of the Reynolds number dependence, or pressure gradient dependence of these features in the boundary layer or in the model.

However, what we have learned so far suggests several critical parameters that can be manipulated to control the production of turbulence and hence reduce the drag. We have focused on the acquisition of additional data to support the rational theory that has been formed, so as to provide the basis for determining how much leverage we have in our efforts to control boundary layer turbulence. We have also continued with a small effort examining some of the controls.

This report is in five parts. A review of the essential structural features of the turbulent boundary layer that are related to the production process; a review of our experimental program to further understand these features and the mechanisms and interactions; a breakdown of the types of local intense interactions of the vortex ring-like typical eddy with the

wall region -- the pocket portion of the bursting process; a discussion of the long range effects of the interaction -- the formation of long streaks and their stability and the formation of secondary hairpins; new two point vorticity correlations that support the presence of typical eddies; and preliminary data on whole field measurements of vorticity etc., using the photochromic grid marking technique. Each part is written as a self contained section.

LIST OF SYMBOLS

D	the diameter of a vortex ring
Uc	convection velocity of a typical eddy
Ur	velocity of a vortex ring
U_∞	freestream velocity
Uw	velocity of the moving belt
δ	the Stokes layer thickness
ν	kinematic viscosity
$( )^+$	non-dimensionalized by ν/u_τ
x	coordinate in the main flow direction
y	coordinate normal to the surface
z	cross-stream direction
θ	momentum thickness of the shear layer
R_θ	Reynolds number
ω_z	vorticity component in the z direction
u_τ	friction velocity
λ	streamwise wavelength

3. REVIEW OF IMPORTANT STRUCTURAL FEATURES

We present a moderately extensive review of the important structural features associated with the wall region events, and then discuss new boundary layer observations that further complete our understanding. Then we present the vortex ring/moving wall simulation experiments, and show where they give us insights and extend our understanding of boundary layer processes. We conclude by briefly discussing the use of the simulation to a) help us further understand the turbulent boundary layer production process, and b) to help establish a rational basis for boundary layer control studies.

3.1. Long streaks found in the wall region

In the discussion that follows, we separate the observation of long streaks, nominally greater than $x^+ = 100$ from the shorter ones, for reasons that will become apparent later.

Early investigations ofRunstadler, Kline and Reynolds (1963) in the near wall region of turbulent boundary layers discussed the existence of regions of both low speed fluid and high speed fluid. In general both regions had a high aspect ratio, being elongated in the streamwise direction. Estimates of the length of the low speed regions, which were marked by a build up of dye they seeped into the sublayer, indicated streaks of 1000 x^+ or more existed. Estimates of the high speed streak length were not obtainable, because they were not marked by dye. High speed streaks were found using Hydrogen bubbles emanating from a wire laid parallel to the wall and perpendicular to the flow. The persistence

time at the wire was considerable, but estimates were not made. The width of low speed streaks was also estimated to be about 20 wall layer units. They found that the high speed streaks were usually wider, and that they extended across the region between a pair of low speed streaks.

3.1.1. Low speed streaks come in pairs

A number of investigators have studied the formation of low speed streaks. Oldaker and Tiederman (1977) observed that a pair of low speed streaks formed as a result of the response to what appeared to be a sequence of local high speed outer region eddies interacting with the wall and aligned along a streamwise direction. The path left by the outer region disturbances clearly formed a high speed streak. Falco (1980a) observed the formation of low speed streaks in pairs by a similar mechanism. Although low speed streaks are often observed to exist singly, care must be taken when interpreting low speed streak formation, because once formed the low speed streaks can persist for very long times (see Smith and Metzler 1983), and have simply convected into the observation zone.

3.1.2. High speed streaks come singly

The formation of pairs of high speed streaks has not been reported, although high speed streaks have been observed to alternate with low speed streaks for short distances near Hydrogen bubble wires. (Short regions of high speed fluid are often observed, and will be discussed below.)

3.1.3. Spacing of the low speed streaks

Schraub and Kline (1965) have determined that the low speed streaks are spaced 102 ± 10 wall layer units. Smith and Metzler (1983) extended the counting to higher Reynolds numbers ($R_\theta \gtrsim 5800$), and concluded that the spacing was Reynolds number independent.

3.1.4. Stability of the low speed streaks

The low speed streaks breakup. This has been observed by all investigators, starting with Runstadler, Kline, and Reynolds (1963). The stability of the high speed streaks has not been similarly investigated.

Low speed streaks have been observed to breakup by first lifting up, then showing a growing waviness, which is followed by rapid breakdown. More recently, Acarlar and Smith (1984) have observed that artificially generated low speed streaks underwent breakdown after they observed the formation of hairpin vortices on top of the streaks. Falco (unpublished) has also observed this form of breakdown of the long streaks, but it was observed less often than the breakdown that follows the movement of the streaks from side to side in plan view (the wavy breakdown of Kim, Kline and Reynolds 1971). Falco (1978) observed another mechanism of long streak breakup that appeared to be most common. Streaks were observed to breakup because of the movement towards the wall of coherent outer region eddies, which simply pushed the marker that gathered into the streak away from their path. Schraub and Kline (1965) also appeared to have observed this form of streak breakup. Looking upstream they observed "the ejection of sublayer fluid appears to be usually initiated by the sudden spreading or widening of a relatively high u-velocity region. This faster fluid then

'interacts' with the slower fluid on both sides as it spreads." They noted that a pair of counter rotating patterns emerged when high speed fluid came down to the wall, pushing low speed fluid -- marked by the presence of Hydrogen bubbles -- sideways.

3.1.5. Reynolds stress

There is very little Reynolds stress associated with streaks that are stably present on the wall. When streaks lift-up, we can get significant Reynolds stress. However, we have observed that the streak lift-up is associated with the presence of a specific outer region coherent motion called a Typical eddy (Falco 1977).

3.1.6. Streak formation

Since the mid fifties, it has been suggested that long counter rotating streamwise vortices exist in the wall region and that pairs of these vortices produce a gathering of wall layer dye between them that we see as the low speed streaks. A high speed streak would be the result of high speed fluid being induced towards the wall between a pair of these streamwise vortices rotating the other way. A number of authors have suggested causes for these streamwise vortices. The currently most popular suggestion is that they are the 'legs' of hairpin vortices that are also observed in the wall region. However, as Acarlar and Smith (1984) have pointed out, is it very hard to understand how the hairpin legs could extend upstream as far as would be necessary to produce streaks of length $x^+ \sim 1000$. Recent full Navier-Stokes calculations by Kim (1986) have indicated that no streamwise vortices of that length exist. Thus, there is

still no experimental evidence supporting the various rational physical hypotheses describing the formation of long streaks.

3.2. Pockets

Another feature of the wall region structure, that is most clearly observed shortly after marker is introduced -- so that the ambient marker is fairly uniformly distributed -- is the frequent rearrangement of marker that moves it away from a local region, leaving a scoured pocket of low marker concentration.

3.2.1. What they look like

Figure 1 shows two pockets as seen in a layer of smoke marked sublayer fluid. Falco (1980a) described the evolution of pockets and conditionally sampled their Reynolds stress and other quantities. The lateral boundaries of each pocket are a pair of streaks. These are low speed streaks, but are much shorter than the low speed streaks (also see Figure 1) discussed above. The existence of both these short streak pairs and of the long streaks led Falco (1980b) to suggest that a double structure existed in the wall region.

3.2.2. Pocket scales

The lateral scale and longitudinal scale of the pockets has been measured. Falco (1983) showed that the lateral scale of pockets when non-dimensionalized by wall layer variables is about 60. Recently, Falco and Lovett (unpublished) have found that this spacing holds to $R_\theta \cdot \simeq 4000$. Thus, the short streaks that form along the sides of the pockets are spaced 60%

of the average of both the long streak and pocket streak spacing. The longitudinal scale of the pockets continues to increase, and at some point in their evolution the apex--where the streaks join--appears to split, leaving two streaks (a pair) of length about x^+ of 80.

3.2.3. Pocket frequency

The frequency of occurrence of pockets has been measured by Falco (1983). The pocket frequency does not scale on either wall layer variables, outer layer variables or a geometric mean of the wall and outer layer variables. It is important to note that they occur, however, far more frequently than the aspect of the bursting process detected by VITA, the currently most popular 'turbulence detector' (see Blackwelder and Kaplan 1976). For example, at R_θ = 2100 Tpu_τ^2/ν = 20, vs. $\gtrsim$100 using VITA. Falco (1980a) showed that VITA detects the situation that occurs during one phase of the evolution of the pockets.

3.2.4. The evolution of pockets

Pockets are footprints of outer region motions that interact with the wall. Falco (1980a) showed that they start out as a movement of wall layer fluid away from a point as a high speed outer region eddy (a Typical eddy, discussed below), nears the wall. The interaction results in the footprint opening up into a developed pocket shape, which has a pair of short streaks at its lateral boundaries. It appears that there is significant vorticity associated with the formation of these streaks (see Falco 1979). Next, fluid is seen to lift-up from the downstream end of the pocket. This lifted fluid takes on the characteristics of a hairpin vortex (Falco 1982).

3.2.5. Reynolds stress associated with pockets

Significant Reynolds stress is associated with all of the stages of pocket formation. Falco (1980a) discussed the distributions in detail. He found that during the early part of the interaction, ensemble averaged Reynolds stress signatures of the order of 10 times the long time average existed, which were the result of the sweep. Later, Reynolds stress signatures of equal magnitude were found that were the result of the lift-up and ejection of fluid from the downstream end of the pocket.

3.3. Hairpins

Vortex lines are constantly being bent in a turbulent boundary layer. When a concentration of these lines has formed, a vortex tube of strength significantly greater than the ambient vorticity can be defined. Although flow visualization of a passive contaminant can not be used to observe vorticity directly, smoke marked features in the wall region that appear to be hairpin vortices have been observed by Falco (1982). The concentration of distorted vortex lines into hairpin vortices has been observed to result from two mechanisms discussed below.

3.3.1. Formation and stability of hairpins emerging from the lift-up of fluid out of pockets

As mentioned above, in the later stages of pocket evolution, wall layer fluid is lifted and at times ejected out of the pocket. This fluid takes the form of a hairpin vortex (see Falco 1982). Depending upon the type of interaction that occurs, the hairpin may a) remain in the sublayer,

b) lift above the sublayer and then return to the wall, c) lift above the sublayer and undergo an evolution that leads to necking down and pinch-off into a vortex ring, or d) lift-up and get ingested into the Typical eddy that induced it up. In general, the hairpins do not remain stable for very long. In particular, we have never observed a hairpin to remain 'intact' long enough to move across the boundary layer as suggested by Head and Bandyopadhyay (1981).

3.3.1.1. Strength of hairpins emerging from pockets

An estimate of the strength of the hairpins that emerge out of the pockets can be made from the data of Falco (1980a) who ensemble averaged the vorticity (as represented by du/dy only) at the downstream end of the pockets at $y^+ \approx 16$. Although this is not a direct measure because the probe is not within the hairpin at its strongest time, and furthermore, the hairpin in some cases has been ingested, it is a conservative estimate. We see that ω_z is four times the mean shear.

3.3.2. Hairpins forming over streaks

We have observed hairpins appearing to form over individual streaks. The streak is seen to become lumpy, and the lumps grow and one or more hairpins appear around these lumps. Acarlar and Smith (1984) have also observed hairpins forming so as to straddle artificially simulated streaks, and it appears, in a turbulent boundary layer. It is not clear how this mechanism works, but it appears to be different from one that involves the distortion of cross-stream vorticity into a hairpin.

3.3.2.1. Strength and stability of hairpins

As far as we are aware, no measurements of the strength of these hairpins has been made. We have made few observations of them. Because of the fact that their formation is likely due to an instability of the streak coupled with the presence of existing streamwise vorticity -- which may be similar to the lumping instability mode found by Swearington (private communication) to occur in some cases of streak breakdown in Taylor Gortler experiments -- and not to the presence of some coherent motion in the region above them, once they form they may not be subjected to strong ambient perturbations that destroy them immediately, and they may move a little further out into the layer. However, as mentioned above, we have never observed a hairpin -- or the smoke marked feature that may indicate a hairpin vortex -- to remain stable and move across an appreciable fraction of a fully turbulent boundary layer. We have observed them to become highly distorted, and, in one case, (Falco 1983) 'pinchoff', and reconnect into a vortex ring.

3.3.3. Hairpin formation at other times

We have also observed hairpins to form between two streaks under conditions in which no pocket was present. Furthermore, we have seen hairpins form at the ends of both long streaks and the short streaks that mark a pocket. Our observations discussed below shed some light on these occurrences.

3.4. Typical eddies

The microscale coherent motions, which are similar to laminar vortex rings embedded in a shear flow, thus described as 'ring-like', are called typical eddies. They have been studied by Falco (1974, 1977, 1983) who showed that they contribute more than half of the Reynolds stress in the outer part of the boundary layer, and that they are the excitation eddies that create the pockets. More recently, Falco (1982, 1983) presented additional evidence showing the existence and importance of typical eddies in the inner region.

3.4.1. Typical eddies are ring-like vortices

All available evidence suggests that the typical eddies are vortex ring-like, i.e., appear to be laminar vortex rings that are embedded in an ambient shear field. Experiments using two mutually orthogonal sheets of laser light enabled Falco (1980b) to determine, as far as the smoked marking allows, that the coherent feature was a ring. Because the smoke does not completely mark the vorticity, it is likely to give an impression of a more sharply defined ring than the actual vortex lines would show. Thus, in a calculation, although one would not expect to find vortex tubes that closed upon themselves without connection to the ambient vorticity, the connection to the ambient should be sufficiently weak so that the dynamics of the localized region would be similar to the dynamics of a vortex ring (which, of course, is entirely different from that of a hairpin vortex).

3.4.2. Typical eddies create pockets

Typical eddies found near the wall are directly responsible for the formation of pockets and play a large part in their evolution. Falco (1982, 1983) and Lovett (1982) have described these interactions. New details about pocket evolution are presented below.

3.4.3. Direction of typical eddy motion

Typical eddies have been observed to move both towards and away from the wall. In general, we have found typical eddies oriented so that they induce themselves away from the wall. However, if they are in a large scale wallward flow, then the net normal velocity component may be wallward. Eddies moving towards the wall have been observed positioned in the valleys between the large scale bulges. Eddies in this position have also been observed to move away from the wall, but most often typical eddies moving away from the wall are found under the large scale bulges, which have a net outward flow (Falco 1977). Most of the observed angles--whether towards or away from the wall--have been shallow, often no more than a few degrees.

3.4.4. Convection velocities

The average convection velocity of typical eddies has been measured in the outer region by Falco (unpublished). It was found that the eddies move with approximately the local mean velocity of the boundary layer at the position of their center of mass.

3.4.5. Formation in the outer region

Typical eddies have been observed to form in the outer region of turbulent boundary layers, on the upstream side of the large scale motions (Falco 1977). Recently, Moin, Leonard, and Kim (1986) have performed numerical studies using the full Navier Stokes equations, and demonstrated that the straining field of a large scale loop of vorticity can induce ambient vorticity to reorganize into a vortex ring. The reorganization takes place on the upstream side of the large scale coherent vortex motion, essentially confirming the observations made in the boundary layer.

3.4.6. Formation from lifted hairpins

Both types of hairpin creation mechanisms described above can produce hairpins that can pinch-off and form new vortex rings. Falco (1983) showed visual evidence of a hairpin lifting from the downstream end of a pocket, contorting and pinching off to form a new vortex ring-like typical eddy. This pinch-off mechanism has also been clearly shown to occur in the calculations of Moin, Leonard and Kim (1986) mentioned above. It is not clear yet which contributes more to the formation of Typical eddies, the pinch-off from pocket generated hairpins, or the pinch-off of hairpins associated with the streaks.

3.5. Streamwise vorticity

Many investigators have noted the presence of streamwise vortices in the wall region. Almost without exception, the vortices have been of short extent (see Praturi and Brodkey (1978), Falco (1980b) Smith (1982)). A number of investigators have suggested that streamwise vortices of much

greater extent exist in the wall region, essentially laying just above the wall in pairs, which are responsible for the creation of both low and high speed streaks. This evidence is of a statistical nature, usually from correlation measurements. However, no one has ever observed them, and recent calculations of turbulent channel flow using the full Navier Stokes equations (see Kim 1986), have shown that the eddies which have streamwise vorticity are not elongated in the stream direction.

4. INTRODUCTION AND OVERVIEW OF THE RESEARCH PROGRAM

A great deal of work is being done to try to control the onset and production of turbulence in boundary layers. However, only vague concepts about the structural features are understood, some of which are wrong, which has led to large scale efforts which don't have a firm foundation. The above review, apart from showing the large number of features associated with turbulence production, also indicates that until the research to be described was done, the connections between various events is only qualitatively established, and no information about the sensitivity of these processes to perturbations, or the possibility of thresholds being involved is known. The engineering devices such as LEBU's and riblets do change turbulence structure, but what they are doing, and how they do it, is currently not understood (in spite of a lot of comments to the contrary). New ideas for control or management of turbulence in boundary layers based on an incorrect or incomplete view of the physics are likely to direct people and resources away from the critical path that will ultimately give us the information needed for a rational approach to control. It appears that fewer resources are being directed at continued

understanding of the phenomena. Although the fundamental research path may appear to result in slow progress, I feel that it is real progress. Furthermore we are embarking upon a period where the use of photo-optical measuring techniques can accelerate our rate of understanding.

In what follows I will review our method of attack and progress in understanding. In my research I am constantly alert to opportunities to control turbulence, and will outreach, doing control related experiments, when there is a identifiable mechanism to attempt to control.

4.1. Our five pronged attack on the turbulence production phenomena

We have been performing a five pronged attack to validate the theory put forth in a series of papers over the past several years, and to obtain new data about the causes of turbulence production near walls. In the course of this period's work new data enabled us to enhance the theory to include all of the important facts. These are described below after a brief review of the essentials of the revised theory. The five prongs are: vorticity-vorticity correlations in a thick boundary layer in air; two view laser sheet/flood light visualization to determine the inner/outer layer interactions; multiple color fluorescent dye marking experiments in water; vortex ring/moving belt simulations in water; and vortex ring moving riblet plate experiments in water. We are, furthermore, developing the photochromic grid marking technique to enable whole field measurements in turbulent and unsteady flows.

4.2. Review of the revised structural theory

The theory has reached a new level of completeness and unification because we have discovered that all of the sublayer perturbations and structural components can be caused by Typical eddies convecting over the wall. The theory says that the major transport occurring in the turbulent boundary layer is brought about by three structural features: the Typical eddies which cause the interaction, the large scale motions which determine the angle of approach of the Typical eddies towards the wall, and the local instantaneous thickness of the sublayer which governs the severity of the interaction. These features can be used to model essentially all of the events that have been observed. The one exception was the formation of the long streaky structure in the wall region. Our new observations have filled this gap.

The key new insight developed as a result of measuring the convection velocity of Typical eddies at various positions across the boundary layer and finding that a large number of them were moving at essentially the local mean velocity of their center of mass. For these eddies, we were talking about .7 U_∞ or greater. Up to this time we had been following the suggestion of Emmerling, Eckelmann, and others who noted that the pressure producing eddies convected at speeds as low as .2 U_∞. A further weak point of the simulation that formed the basis of our model was our association of the edge of the Stokes layer with the edge of the viscous sublayer. Thus, in our simple Galilean transformation, we assumed that $Ur/Uw = 1 - .5\ Uc/U_\infty$. As a result, our simulations modeled Typical eddies that moved $0 < U_\infty < .5$, whereas our new measurements show that the majority of the Typical eddies are moving faster. The faster moving eddies exert an

influence on the wall from a greater distance than we had previously witnessed. They also result in a far field interaction that produces pairs of the long streaks. Investigators have been observing similar streaks since the early studies of Hama and Kline. The fact that interactions can take place at a greater distance from the wall allows a greater number of eddies to be involved. In Part II we describe the experiments that provided the new data. Because of the need to have high resolution to define details of the local interactions as well as encompass the long distance interactions, a number of different techniques had to be used. In what follows we summarize the emerging overall picture.

Typical eddies, which are essentially Taylor microscale size vortex rings, are created by vorticity redistribution in the outer layers near the upstream side of the large scale motions, and by pinch-off of lifted hairpin vortices. While both of these processes have been observed, in a) the fully turbulent boundary layer, b) vortex ring/moving wall interaction experiments, and c) full Navier-Stokes calculations (Moin, Leonard and Kim, Phy Fluids April 1986), they are not yet fully understood, and experiments are proposed below to gain an understanding. It is in modifying these processes that we have the greatest chance of controlling boundary layer turbulence. The Typical eddies are convected over the wall in the speed range of $.2 < U_\infty < .95$, but most of them move faster than $.7\ U_\infty$. We will, at this point, define a fast Typical eddy, somewhat arbitrarily, as one moving with $Uc > .7\ U_\infty$. When we investigated the interactions possible with the faster eddies in our vortex ring/wall simulations, we immediately witnessed the other aspect of the turbulence production problem, i.e., the appearance of long streaks and their breakup. This is the aspect most other

investigators have concentrated upon. Thus, we now have in one structural model the two most important features of the production of turbulence. Previously it had appeared that two different mechanisms would be required, but only one is seen to be needed: the Typical eddy wall interaction. The high speed Typical eddies cause a rearrangement of the wall layer fluid into streaks that are spaced approximately the diameter of the eddy. Since the distribution of eddy sizes is lognormal, with its mean around 100 wall layer units in low Reynolds number boundary layers, we immediately have the basis for the streaky structure scaling. The Navier-Stokes equations indicate that we can generate streamwise vorticity near a wall by the presence of a spanwise pressure gradient. Thus, we do not need the pre-existence of streamwise vortices in the model. This certainly removes one of the sources of mystery from the boundary layer. Thus, it is clear for a given δ/D as we cover the range of convection velocities, we can uncover the range of interactions the coherent outer layer motion can cause.

Additional measurements in the turbulent boundary layer indicated that zero degree angles were not uncommon and that some Typical eddies had negative angles (they were moving away from the wall) while the interactions were observed.

If the Typical eddy is in the correct speed range to produce streaks, then the absolute distance from the wall, the thickness of the wall layer, the eddy size, and the angle of incidence determine the ensuing <u>stability</u> of the streaks that are formed. All other parameters held constant, if the eddy is moving parallel to the wall and its distance from the wall is greater than some critical value--but not too far, long stable streaks are created. If its distance is less, a pair of streaks starts to form, but it

never stabilizes, and is observed to immediately become unstable, with the initial streak pair bifurcating several times into additional streaks, which all undergo wavy breakdown, and quickly leave the appearance of a turbulent spot forming in the wall region. This process, which has not been observed before to my knowledge, depends upon the Typical eddies' speed, size, distance from the wall region, and the thickness of the wall layer. Experiments have shown that $h_1/\delta < 3.5$ for a visually detected interaction, where δ is the edge of the viscous region or $y^+ = 30$. Thus, in our analogy, any Typical eddy within $\approx$ 135 wall layer units from the wall will create the long streaky structure, and this structure will remain stable long enough to form a quasi parallel pair.

The role of the thickness of the sublayer must be reassessed again in the light of the new range of findings. We have observed that the time to breakup of the long streaks that do so is longer in thicker wall layers. They sometimes appear not to breakup at all. When they do, the mode of breakup is different. In a thin layer the streaks break up by undergoing what appears to be a growing waviness (for opposing viewpoints see Kim, Kline and Reynolds (1971), Falco (1980b)). In a thick layer, the streak breakdown is via a mechanism of lumping up being associated with the formation of hairpins straddling them.

The size and the angle of incidence of the Typical eddy are important parameters determining the nature of the interaction. An interesting fact is that under constant ambient conditions, for eddies of shallow angle, there is also a critical <u>size</u> above which the interaction is massively unstable, resulting in the breakdown becoming a 'turbulent spot' mentioned above. Just decreasing the size is sufficient for the streaks to form and

remain stable. As the eddy gets closer to the wall, it creates a pocket, and may undergo the Type I, II, III, or IV interaction (reviewed and extended below).

The massive instability may be the most violent interaction to occur in the turbulent boundary layer. Falco (1977) called interactions which had this character 'superbursts'. These are bursts that are considerably larger and involve finer scales within them, and occur one tenth as often. With our current understanding, it now appears that the distance from the wall is as important as the angle of incidence. Large scale inflows that can bring the Typical eddy close enough to the wall can cause interactions ranging from minor rearrangements to a superburst! Thus, large scale motions play an even more critical role than previously thought, since it now appears that there is some critical distance from the wall which, if they can convect the eddy to that distance, can result in strong vs. weak interactions. So, a change in the strength of large scale sweeps can keep a host of Typical eddies out of the interaction range.

Since the size of the Typical eddy is a function of the Reynolds number -- the Typical eddy decreases in size with respect to the boundary layer thickness, but increases with respect to wall layer scales, as the Reynolds number increases -- those interactions depending upon the outer scale size will decrease in number and strength, while aspects depending upon the wall layer scaled size will increase. So, for example, the occurrence of superbursts may increase, and the spacing of streaks may also increase, or streaks may disappear altogether because conditions for their stability no longer exist. An understanding of how to non-dimensionalize the parameters of size, distance from the wall, and wall layer thickness

needs to be gained.

It should be pointed out that the streak breakup does not appear to be a simple shear layer instability in the normal sense, which depends upon the local shear layer thickness and the velocity difference. In simulations of streaks formed by vortex ring/wall interactions, we could keep the velocity difference the same, keep the shear layer thickness the same, but create streaks that were very stable.vs. streaks that were immediately unstable, by varying the size of the ring by an almost immeasurable amount.

A subset of Typical eddies which are in the range $h_1/\delta < 1.7$ -2.0 and are moving very slowly, .2-.4 U_∞ will form a hairpin vortex at the downstream end of the interaction region from which a streak pair was initiated, if the incidence angle is very shallow, and this hairpin can lift up and pinch-off, forming a new vortex ring/Typical eddy.

In general, however, the Typical eddies that move slower interact over a more local region. They do not produce the long streaks or the extensive wall layer breakup. Their disturbance is organized around the pocket footprint. Fast eddies, which exist farther out, will produce streaks and pockets, while the slower moving Typical eddies which are closer to the wall will produce only pockets.

We have also observed Typical eddies that clearly produce a Type II interaction which are more than one diameter from the wall, i.e., they produce large clear pockets and no streaks, and they remain stable and have a hairpin liftup from the pocket, which goes back down to the wall. These eddies are moving slowly so they represent fluid that has recently moved quite far from the wall, and/or formed a strong Typical eddy that is inducing itself in the upstream direction against the mean flow.

With our new information and understanding of the far field effects of the Typical eddy, it has become clear that we have a broader range of interaction producing turbulence that must be classified. The new classification is in the order of increasingly strong interaction: no interactions of any type occur if $h_1/\delta > 3.5$. We must now consider both the stability of the ring and the stability of the streaks in all cases. We will organize the classification around Typical eddy speed. Organizing around speed, we can keep the four Types previously identified (and reviewed below), but need to add six additional, which involve the streaks, and the superburst.

The four types previously identified which involve local interactions all involve slow speed Typical eddies moving towards the wall:

Type I -- Interaction results in a pocket, which has a weak liftup at its downstream boundary which results from induction by the Typical eddy, that is confined to the wall layer ($y^+ < 30$). The eddy leaves the interaction intact. It results from very low speed Typical eddy moving at shallow angles, and the sublayer must be thick. The probability of this is very low, primarily because of the low probability of an eddy having this speed.

Type II -- Interaction results in a pocket, which has a strong hairpin lift out of it downstream boundary as a result of induction by the Typical eddy. This hairpin moves beyond the wall layer. No fluid is ingested into the ring, which remains stable as it moves away from the wall. These interactions have been observed for eddies moving towards the wall at shallow angles.

Type III -- A Typical eddy moves towards the wall, and interacts creating a pocket. The hairpin liftup induced by the Typical eddy at the downstream boundary of the pocket is partially ingested by the eddy. This ingested fluid causes the eddy to become unstable and it breaks up as it moves away from the wall. The wall layer must be thin and vortex stretching, due to inviscid image effects, dominate the physics.

Type IV -- Interaction results in a pocket, and liftup induced by the Typical eddy, that is almost completely ingested into the eddy which is strongly stretched as it gets close to the wall in a thin wall layer. Both the eddy and the lifted ingested fluid breakup in the near wall region.

We now discuss <u>non-local</u> interactions resulting from Typical eddies convecting at speeds > .7 U_∞.

Type I(S)-IV(S) -- Typical eddy moving towards the wall at a shallow angle produces a pair of parallel streaks followed by a Type I - IV interaction as the eddy gets closer to the wall. A further breakdown is not possible at this stage. We need additional experiments to uncouple the dependence of the angle of incidence, and the various scales, to understand why at times the pair of streaks will be stable, and at other times they will become lumpy or wavy and breakdown. Clearly the angle of incidence is an important variable. We have further observed that the time to instability of those streaks that do become unstable is longer in a thicker wall layer.

Type V -- Typical eddy moves toward the wall at a shallow angle and starts to produce a pair of streaks. However, from their inception these streaks do not have a definable spacing, but continue to move apart, then they bifurcate, producing other incipient streak pairs that are also not

stable. As the third pair is forming, the first pair is undergoing wavy breakdown; soon all the streaks are breaking down and include the pocket that forms by about the time of the first bifurcation. The overall breakdown strongly resembles the growth of a turbulent spot. This can occur with the Typical eddy undergoing a Type II to Type IV interaction. I do not feel that this event should be classified as a low speed streak pair instability, because streaks only begin to form and never attain a stable state from which to go unstable. The interaction should be looked upon as whole. An additional type of interaction has been observed that does not classify according to eddy convection velocity.

Type VI -- Typical eddies moving at very shallow angles to the wall. If the convection velocity is <u>low</u> ranging from $.1 < U_\infty < .4$, it will induce a hairpin vortex of lifted fluid trailed by a pair of long, very stable streaks. If the angle is towards the wall, the lifted hairpin has been observed to pinch-off and form a new vortex ring. If the angle of flight is away from the wall, the hairpin doesn't pinchoff. In this interaction a pocket may not form. The streaks are close together when the Typical eddy is far away, but moving towards the wall, and progressively spread if the eddy starts closer to the wall. This is a case where the effect of angle is greater than the effect of convection velocity. The probability of occurrence is relatively high because it represents the case where a Typical eddy is evolving from a hairpin that has lifted from the sublayer and has recently undergone pinchoff. Both the ring stability and the streak stability depend on the layer thickness, but the streaks first develop into long parallel pairs before any instability sets in.

As we can see, the importance of a thick sublayer in reducing the intensity of the turbulence production is clouded by the presence of these additional poorly understood interactions. It is, of course, still of great importance for slow moving eddies, but the faster moving eddies will make an important contribution to the momentum transferred by creating long streaks that may become unstable. We have two tasks before us. First, we must determine the frequency of occurrence of each of the types of interaction; and second, we need to determine the parameters that govern the stability of the different types. Determining the frequency of occurrence will require a number of different techniques of flow visualization, as discussed in the next section, but it is clear that some of the interaction types discussed above will not be frequent in low Reynolds number flows, although we suspect the situation at higher Reynolds numbers may well be different.

Determining the parameters governing the occurrence of a particular type of interaction in the fully turbulent boundary layer is very difficult because we need to measure all relevant parameters, in a environment where several interactions may be occurring at the same time. Our current procedure involves continuous observation of the turbulent boundary layer until those times in which essentially only one type of interaction is occurring in isolation. We then measure various parameters with hot-wire anemometers. We have, of course, been helped in an important synergistic manner by insights from our vortex ring/wall simulations. Experimentally, a major increase in our ability to determine the governing parameters will result from being able to quantitatively follow the evolving flow in two dimensions. Being able to make measurements as the flow evolves means that

we will relax the constraint of exact phasing of the turbulence with our instruments. Furthermore, we will be able to measure quantities like the vorticity and strain-rate over a field, so as to understand questions of the sensitivity of interactions. This will essentially put our capability on a par with low Reynolds number Navier Stokes Equation computational work in channel and pseudo boundary layer flows. It does not overcome the problem, common to both approaches, that in the boundary layer a number of production events, in different stages of their evolution, may have an effect on the measurement area at the same time. (We will have the advantage of larger ensembles, but more limited data, and the capability to increase Reynolds number, but I foresee a strong synergism developing between the two.) Experiments are currently being set up to enable such measurements to be made.

A second important point is that it is now clear that making a 1-1 correspondence between all the streaks that form and coherent motions that exist in the flow above the wall is not possible. This is because of the observation that more than one pair of streaks can result from a single Typical eddy interaction, especially if the speed ratio Ur/Uw is greater than .35. Obviously, if a portion of a streak created by the bifurcating(multiplying) mechanism is in the streamwise/normal laser sheet, we would not find a Typical eddy or any other coherent motion above it (upstream or downstream).

The breakdown helps to point out that there appear to be essentially two ensuing streak instability mechanisms, the wavy breakdown, and the lumpiness which evolves into hairpin vortices. The cases where streaks form and are initially stable, but then undergo rearrangement through lumpiness

or wavy breakdown, do result in additional turbulence production, but it is weak, and I have characterized it as slow production, in contrast to the Type II-IV interactions or the Type V interaction. The existence of the streaky structure contributes to the production of turbulence in the following ways:

a) it lifts fluid away from the wall, bringing it into closer contact with the vortices further out, so they can induce continued outward motion;

b) the long streaks appear to become unstable in the lumpy mode, which is associated with the formation of hairpin vortices straddling the streaks, which move away from the wall.

We have observed that this mode of instability occurs more often when the wall region is thick. It is important to put these hairpins into perspective. They very quickly get contorted, and some may undergo pinchoff, forming new vortex rings. All of them act to lift some of the fluid in the streaks off the wall, thus contributing to a local streak liftup. This lifted fluid seems to get moved around quickly along with the contorting hairpin. This qualifies the event to be called a breakdown of the lifted streak, and appears to be the mechanism that Kline et al (1967) hypothesized. However, our observations suggest that it is not likely that these hairpins are responsible for the creation of the long streaks. They are also not likely candidates for the intense high speed sweeps ('q4' events). Furthermore, the liftup that they produce is only a small fraction of the overall liftup of low speed fluid ('q2' events) that is part of the bursting process. And finally, they are not observed to get stretched and

propagate across the boundary layer to form the large scale eddies as conjectured by Head and Bandyopadhyay (1981).

c) they can become unstable by developing a growing wavy instability that amplifies and leads to a wispy fragmenting of the dye in the streak over a fairly long time scale (low production rate),

d) they locally thicken the sublayer, promoting weaker Type I and II interactions when new eddies interact over them,

e) their formation locally thins the sublayer in regions between the low speed streaks enhancing stronger interactions of Type III and IV, when new eddies interact over the high speed regions.

Finally, observations clearly show that in the low Reynolds number turbulent boundary layer there is a predominance of well defined pockets. This follows, because in almost all the cases of interaction, pockets are a part of the events. At times we have also observed several pockets in a row resulting from one Typical eddy.

4.3. Correspondence with full Navier Stokes calculations

During the course of this past year, two of the key observations that are fundamental to our picture of the turbulent boundary layer have been confirmed by supercomputer calculations performed at NASA AMES using the full Navier Stokes Equations (P. Moin, Bull. APSDFD 1985 p 1723; and Moin, Leonard and Kim, Phy Fluids 29 April 1986). The first correspondence shows that the pockets are the essential Reynolds stress producing event in the wall region. The second set of calculations have shown that vortex rings can be generated by two mechanisms present in turbulent boundary layers. The first is by 'pinchoff' of lifted hairpin vortices, and the second is by

redistribution of diffuse vorticity at the upstream side of a large scale concentration of vorticity that resembles a large scale motion. The calculations, while confirming these underpinnings of our theory, can also be used to enhance our understanding of the physical circumstances that cause them.

4.4. Predictions based on the structural model

Two types of predictions arise out of the findings. One is that there is a Reynolds number dependence of the streaky structure. I am not only talking about the streak spacing, but I am more fundamentally referring to the existence of the long streaks. The other is that we should expect structural differences in channel flows.

4.4.1. Reynolds number dependence of the production process

At high Reynolds numbers, the Typical eddies increase in size with respect to the sublayer thickness (Falco 1977). Thus, the interactions that would result in stable streaks at low Reynolds numbers would cross the stability boundary, and result in an interaction in which long stable streaks would not form at higher Reynolds numbers. Thus, we would have a different picture of the balance of streaks and pockets at higher Reynolds numbers. In the extreme, at very high Reynolds numbers relevant to technologically important flows, we may not see long streaks at all.

The strength of the large scale motions also increases with Reynolds number. Therefore, the angle of incidence of the Typical eddies caused by the large scale wallward sweeps will be lower at low Reynolds. Our simulation experiments show that, other conditions held constant, if the

angle is reduced, more long, stable streaks will form. Thus, we expect that at higher Reynolds numbers, fewer streaks will form. Thus, we expect that the streaks will not be a significant part of the wall layer structure at high Reynolds numbers.

Recently, Smith (1983) extended streak spacing measurements to R_θ = 5830, and concluded that the spanwise distribution of the streaky structure did not change appreciably, and that the appearance was essentially the same. He suggested that this would be the case for higher Reynolds number flows. Two points should be mentioned. First, Hydrogen bubbles only give visual information in the region close to the bubble wire, and thus, the observer can't tell whether he is observing long streaks or short streaks. Short streaks are developed along the sides of the pockets, and are the order of 100 x^+, so appear exactly as the longer streaks in Hydrogen bubble experiments. Second, the change in scale of the Typical eddies is slow, so that it may require another order of magnitude increase in Reynolds number to begin to see the effects.

4.4.2. Channel flow differences

The second prediction concerns the difference between channel flows and boundary layer flows. For many years it has been observed that the burst rate indicators in channel flows give different results from those in boundary layers. Because of the flatter 1/7 power profile, the convection velocity of the Typical eddies will be higher, and it is furthermore the case that the angle of incidence is flatter, because the large scale sweeps are not as strong as in a boundary layer. Therefore, the likelihood of

Typical eddies creating stable streaks should be greater in a channel than in a boundary layer.

5. EXPERIMENTAL TECHNIQUES

5.1. Boundary layer measurements and observations

The boundary layer motions were made visible by seeding the flow with .5 - 5 micron oil droplets, and illuminating the oil fog with laser light spread into sheets that could be placed parallel to the wall in the wall region, or perpendicular to the wall and parallel to the flow, or both. The technique has been described by Falco (1980c), so we will not repeat the details here. A new twist used in these new experiments, which was of particular value in finding the long streaks and their correspondence with the coherent motions above the wall, was the capability to observe the washout of smoke in a laser sheet parallel to the wall while we could simultaneously observe the motion above the wall in a laser sheet perpendicular to the wall and parallel to the flow. The experiments were performed in either a 56 foot long working section boundary layer tunnel, or a 24 foot long tunnel. Both had cross-sections of nominally 2 x 4 feet. For these experiments two lasers were available, a 40 watt Copper vapor laser and an 8 watt argon ion laser.

Measurements were also made in a 20'x3'x.5' water tunnel, using red and green and yellow fluorescent dyes.

The vorticity probes used were designed according to Foss, Klewicki and Disimile (1986), and consisted of four one millimeter 5μm tungsten wires, two which are parallel and 1mm apart and two in an x configuration

(also 1mm apart). The center of the x and the parallel wires was 3.5mm apart.

The hot-wire measurements were recorded using a Data Translation simultaneous sample and hold 12 bit 16 channel A/D converter (DT3368/DT3369), and recorded on magnetic disk using a PDP11/73 micro computer. The long records needed for correlation measurements and statistics of vorticity were obtained with the help of double buffering. The data was reduced, in part, using the College of Engineering VAX cluster.

5.2. Vortex ring/moving wall simulations

We can simulate the interaction of a typical eddy with the viscous wall region of a turbulent boundary layer by creating a vortex ring and having it convect towards or away from a moving wall. For convenience, we have used an impulsively started wall. It has the advantages of being an exact solution of the Navier-Stokes equations (Stokes first problem), and therefore is well defined. Furthermore, the velocity profile is approximately linear in the wall region which is similar to the mean velocity profile of the viscous sublayer of a turbulent boundary layer. It is relatively easy to match the friction velocity in these simulations with those found in low Reynolds number turbulent boundary layers. We can also match the Reynolds number and relative convection velocity of the typical eddies.

5.2.1. Experimental apparatus

Experimental simulations were performed in a water tank which is 16" deep by 12 3/4" wide by 96" long. Figure 2 shows the side view and end view of the experimental apparatus, which includes a vortex ring generating device, a moving belt and driving arrangement, a synchronizing timer, and visualization recording devices.

The vortex ring generating device includes a constant head reservoir from which fluid, which could be dyed, passes through a solenoid valve whose opening time could be varied, and an orifice of prescribed size (see Figure 2 items 1,2,3). The constant head reservoir (item No. 1) is filled with a mixture of 10 ppm Fluorescent Sodium Salt Sigma No. F-6377, green dye and water solution. As the solenoid valve (No. 2) opens, a slug of dyed fluid is released from the orifice (3) by the pressure head, and rolls up into a vortex ring. Three different inner diameters of the oriface have been used; 1", 1/2", and 3/8". The size and speed of the vortex ring generated depends upon both the height of the dye reservoir and the opening duration time of the solenoid valve for a fixed orifice. The details were discussed in Liang (1984).

The wall upon which the vortex ring interacted is actually a moving belt (4) made of transparent plastic which has a smooth surface. Two ends of the belt are joined together to form a loop, which circulates around two rollers (5) as shown in Figure 2. The width of the belt is 7 inches; and the distance between the two rollers is 60 inches. The test section is at 30 inches downstream from one of the rollers, giving us a Stokes layer for this distance (if the belt is run longer, Blasius effects begin to enter into the problem). This width/length ratio is sufficient to prevent the

disturbances generated in the corners from reaching the center of the belt at the test section. Therefore, the wall layer flow on the moving belt could be considered two-dimensional. One of the rollers is driven by a 1/4 HP DC motor (6). The speed of the belt is adjustable within the range from 1 in/sec. to 9 in/sec. The belt reaches a constant speed very soon (within a second) after power is on. This short acceleration period allows us to consider the belt to be impulsively started. As the belt moves, a Stokes layer builds up on the belt. A mixture of red food coloring and water is used to mark the wall layer for visualization. The belt is covered with dye before each run during a 'dye run' using a dye injector near the leading roller of the belt, shown in Figure 2 (7). The fluid is allowed to come to complete rest before each 'data run'.

The opening duration time of the solenoid valve, and the time delay between the onset of the belt movement and release of the vortex ring are controlled by a 115 VAC/60 HZ timer designed in the laboratory. Since the thickness of the Stokes layer, δ, is a function of the square root of the belt run time, by carefully adjusting the time delay, we can adjust δ/D as desired.

The primary visual data consisted of simultaneous plan and side view time resolved images which were collected using a standard video camera, a VCR, and a monitor, are shown in the end view of Figure 2. The side view was often illuminated by a laser sheet emitted from an 8 W Coherent CR-8 Supergraphite Argon Ion Laser. The visual data were analyzed on a high resolution monitor with a superimposed calibrated scale, using the slow motion capabilities of the recorder. A limited number of three view experiments were made, in which a laser sheet cross-stream view was added.

6. RESULTS FROM THE FIVE SYNERGISTIC RESEARCH PROJECTS

The five prongs are complementary attacks on the problem of understanding turbulence production. We have found that advances in our hypotheses have required us to go back and forth examining data obtained from the different techniques available in the laboratory, as well as to have the capability to choose the technique that is best when new data is needed to answer specific questions that arise.

6.1. Correspondence between spatial correlations and coherent structure information in a turbulent boundary layer

Two 4-wire cross-stream vorticity probes have been used to obtain vorticity distributions and two-point spatial correlation measurements across the turbulent boundary layer. There are two main goals to these experiments. First is to determine, for the first time, the statistics of vorticity across the entire layer, with special emphasis in the near wall region. Second, to determine whether two-point spatial correlations of vorticity can reflect the coherent structure picture that conditionally sampled measurements are suggesting.

6.1.1. New findings using hot-wire anemometry

Distributions of the streamwise and normal velocity fluctuations, the Reynolds stress, and the vorticity and strain-rate, as well as the skewness and flatness of these quantities, have been measured at three different Reynolds numbers. Of particular interest, we have obtained data as close as $y^+ \approx 4.6$, and thus have the first data in the sublayer and lower part of the buffer layer. Since it is essentially impossible to obtain vorticity

data this close to the wall (we required a 56 foot long wind tunnel), the information is extremely valuable both for the information it conveys, and because it represents a data base against which to check numerical computations. Figures 3 and 4 show the skewness and flatness of v. The v statistics have been measured close to the wall by a number of investigators. The skewness of v shows good agreement with the measurements of Andreopoulos, Durst, Jovanovic and Zaric (1984), but disagreement with the computations of Kim, Moin and Moser (1986) near the wall, where the computations show opposite trends. We performed the experiments at three Reynolds numbers ranging from R_θ =1010 to 4850 to determine if these differences were due to Reynolds number effects. Although it is clear that there are strong Reynolds number effects in the outer region, in the wall region we can see that the differences are not due to Reynolds number effects.

Looking at the flatness of v, we see that our data agree well with those of Andreopoulos et. al. (1984) in the log region, and their Reynolds number dependence in the outer region is consistent with ours. The computations of Kim et. al. (1986) show values of the flatness which are very much higher in the wall region, suggesting that in the computations there exists a narrower range of events and some extremely large events that don't show up in the experiments. Figures 5, 6, 7 show the rms, skewness and flatness of the cross-stream vorticity. Our measurements indicate rather good collaspe of the rms ω_z across most of the layer, when scaled on wall variables. Agreement with measurements of Balint, Vukoslavcevic and Wallace (1986) (who used a nine wire probe) for $y^+ > 15$ is very good. The agreement with the nine wire probe indicates that cross-

flow velocity errors, which any four wire probe can't correct for, are not important. In the near wall region, our measurements show that rms ω_z increases more rapidly as we approach the wall than the computations of Kim et. al. (1986).

The skewness of ω_z shows Reynolds number similarity in the wall region $y^+ < 40$, and a Reynolds number dependence in the log and outer regions. The data of Balint et. al. agrees well in both of these regions. The decreasing skewness as we move closer to the wall than y^+ about 40, is most unexpected. Computed statistics are not yet available for comparison.

The flatness of ω_z (Figure 7) also shows remarkable similarity in the wall region ($y^+ < 40$). It to shows the strong Reynolds number dependence in the log region as well as the outer region. There is some evidence in both the skewness and flatness data that for Reynolds numbers above 2000-3000, a rough similarity may develop in the log and outer regions.

Thus, the skewness and flatness of v and ω_z have a number of supprises and show important differences from the calculations of Kim et. al. We hope that comparisons of this type will enable us to more critically compare the capabilities of direct numerical simulations to uncover the physics of the turbulence production process.

6.1.2. Vorticity-vorticity correlations

Two-point cross-stream vorticity correlations were made. One vorticity probe was held fixed at $y^+ = 15$, and the other above it was moved across the boundary layer. Data records of 600,000 points were used in the correlations. Figure 8 shows the results (Klewicki and Falco 1986) superimposed upon a sketch of a Typical eddy. We see that the correlation

is strongly negative at $y^+ \simeq 40$. For this to be the case, the lower probe must be in a region of strong negative fluctuating vorticity (the sign of the mean vorticity), and the upper probe must be in a region of strong positive vorticity at the same time. This is precisely what happens when a Typical eddy is inducing a hairpin as shown in the sketch. The sketch is to scale of the average eddy, and thus the secondary weak positive between $y^+ = 75$ and 125 is also expected. This evidence is the first long time averaged statistical evidence to support the hypothesis of vortex ring/like Typical eddies as the initiator of the turbulence production process. The magnitude of the correlations further suggests the high frequency of the event.

6.2. New visualization of the inner/outer layer interactions

Both 16mm and 35mm movies have been made of the visualized turbulent boundary layer at low Reynolds numbers to answer questions that remained unclear about the structural features of the turbulent boundary layer.

6.2.1. Pairs of long streaks are observed to be formed by Typical eddies

Using the smoke washout technique using a single laser sheet parallel to the wall, and two mutually perpendicular laser sheets, the washout is observed only in the confines of a laser sheet that is parallel to the wall and extends from the wall to about $y^+ = 15$. The laser sheet focuses attention on the wall for the entire field of view, whereas slit marking/flood illumination soon masks the wall, because the marker is convected away from the wall, obscuring the wall events. We found that the long streaks would last a very long time on average, suggesting that the

near wall region of the streak is not involved in the breakup. We also found that pairs of streaks could be observed to evolve, which sometimes had a pocket form at their downstream end.

Using two mutually orthogonal laser sheets, we found that Typical eddies which where quite distant from the wall (distances greater than their diameter) could create a hairpin lift-up at the wall. If they convected essentially parallel to the wall, or moved outward, they produced a pair of long streaks which were quite stable as viewed in the laser sheet parallel to the wall. These interactions did not result in a pocket forming. These eddies were on average moving at speeds close to the local mean velocity, putting them in a range $.7 < Uc/U_\infty < .9$. Typical eddies that were also as far from the wall, but which moved towards the wall, could also be seen to produce pairs of long streaks. However, these culminated as the eddy came closest to the wall by forming a pocket, which opened up at the downstream boundary of the streak pair. When the pocket formed the streaks were more often unstable.

Isolation of the parameters involved was only possible in the vortex ring/wall interaction simulation experiments described later, which were used to determine the sensitivity of parameters involved in these streak formation events.

Although the laser sheet/smoke washout technique is very informative, it can't be used to build up significant sample sizes, because each experiment reveals information for only the very brief period during which the marker goes from high to zero concentration. In practice this has meant data over about two boundary layer thicknesses. Thus, the odds of catching the events of interest in the two laser sheets during this short time are

low, and thus an impracticably large number of experiments would be needed. We have, instead, started a different approach, using fluorescent dyes and multiple sublayer slits in a water tunnel, which is described below.

Another new aspect of the interaction was observed in these movies. We found that a single Typical eddy could produce more than one pocket. This occurred when the eddy was on a shallow wallward trajectory, from which it created a pair of long streaks, with two (sometimes indication of three) pockets which were roughly in line between the streaks at their downstream end. The formation of the pockets, with their hairpin lift-up, marked the culmination of the interaction. No additional wall disturbance was noted downstream.

Thus, only one coherent motion, interacting with the wall, is necessary to create both the long streaks and the pockets. Since all of the remaining structure found in the wall region is related to these two structures, we can say that the typical eddy is responsible for the onset of the turbulent production process.

The long range effect of the Typical eddy upon the wall region leading to the streaks has made the observations connecting the formation of a streak pair with the passage of a typical eddy very difficult. For a long time the connection was dismissed, because it was thought that other motions (for example, the large eddies) or other mechanisms within the boundary layer must have had the governing influence, and here we include any of the classical hypotheses. However, using the vortex ring/moving wall model, we found that the interaction of the coherent vortex rings definitely does occur over these distances. With the model, which doesn't have any additional influences present, we could be certain that the

interaction was the effect of the passage of the eddy. This evidence does not remove the possibility that other coherent motions in the boundary layer can create a pair of long streaks; however, Falco (1977, and recent unpublished information) has pointed out that there are only two important coherent motions, the typical eddies and the large scale motions. This, combined with the fact that if all other scales of motion in the boundary layer contributed to the creation of streaks, we would not have a preferred streak spacing of approximately 100 wall units (Schraub and Kline 1965), lends support to the argument that typical eddies are primarily responsible. The possibility of interaction of the large scale motions cannot be ruled out, but at high Reynolds numbers the large scale motions may have scales many thousands of wall layer units, and thus could not be the primary streak producing mechanism.

6.2.2. All occurrences of hairpin vortices connected with typical eddy/wall interaction.

Observations mentioned above have indicated that hairpin vortices can form as a result of pocket evolution and as a result of lumping instability of existing low speed streaks. We also indicated that there were occurrences where neither of these mechanisms appeared to be the cause. We have now identified another mechanism that can result in the formation of hairpin vortices. When a typical eddy is moving away from the wall at a shallow angle and when it is moving relatively slowly, say $Uc/U_\infty < .4$, it will create a pair of long very stable streaks that trail behind a hairpin vortex that lifts-up slowly. The eddy can be as far from the wall as indicated above, and thus, will convect appreciably downstream before the

hairpin will be noticed. It may convect out of a field of view, leaving the observer with the impression that the formation of the hairpin did not involve the coherent motion.

The fraction of the remaining hairpins that this accounts for is not known, but it may well be an important percentage.

6.2.3. Pinch-off of lifted hairpins

Falco (1983) has previously observed the pinch-off of a lifted hairpin vortex. This observation required two perpendicular laser sheets, two smoke slits, and selective filtering of the laser light, and sufficient light intensity and film resolution to cover a field of view of several boundary layer thickness, plus receiving optics to align, and enable split screening of the two views. Even with this arrangement, the circumstance of the characteristics of the excitation eddy could not be ascertained because it was not in the laser sheet illuminating the flow above the wall at the time the pocket was formed. It will be very difficult to detect, and almost impossible to quantify this process, without the aid of two-dimensional, and even three-dimensional quantitative Lagrangian measurement techniques.

6.2.4. Determining the Type of Typical eddy wall region interaction.

Using dual wall slit laser and flood light visualization of boundary layer and two mutually orthogonal viewing planes, we obtained new results that covered a field of view consisting of the entire boundary layer. This was possible because of the availability of a 40 watt copper vapor laser. Smoke was emitted from one slit far upstream filling the entire boundary layer, and from a second slit in our field of view. This technique can help

to confirm the findings of the last section, but, whereas the washout technique allowed streaks to be seen most clearly, the slit enabled us to view pockets most clearly. With this experiment we focused on trying to build up a larger sample of events, with clearer information about the typical eddy/wall interaction. Note, the question of whether Typical eddies have caused the long streaks can't be determined by this technique, because we don't have information upstream of the slit, and the lifted fluid quickly 'clouds up' the picture downstream as we look downstream of the slit.

6.2.4.1. Majority of the interactions at R_θ = 1000 are Type II and III

One of the important goals of our visual investigation was to build up a large enough sample to enable us to determine which one of the four types of local Typical eddy wall interaction was most common. We analyzed 10 rolls of film (10 runs at $R_\theta \lesssim 1000$ and found that it is either Type II or Type III interactions that are the most common. The problem with getting a more definitive answer is that we could not separate marked fluid once it was lifted (since it is all white oil droplets) to determine a) if it originated from the sublayer, b) if some of it entered the evolving Typical eddy or not, except for some occasions where concentration gradients were accidentally present. Although observations when mother nature permitted were enough to understand the presence of the phenomena, we could not build a statistical sample on this basis. This state of affairs, combined with the desire to see whether or not the situation was different in the cases when streaks formed upstream, has led to the multiple color dye water tunnel experiments which are still in progress. As a result we have not

counted the number representative of each catagory. However, we can also say that Type IV events are quite rare at R_θ = 1000.

6.2.5. The pocket as wall phenomena

A number of experiments using artificially generated hairpin vortices have suggested that the pockets observed by myself and others are structures that exist well out into the boundary layer, and are thus, by implication, not the wall phenomena suggested, but simply the visual pattern one would see under the legs of a tilted hairpin vortex. We wanted to show that the influence actually extended into the sublayer and to the wall. This was demonstrated by the following experiment: A surface with very low shear modulus and very low damping was installed in a kerosene flow channel. Because of the index of refraction of kerosene over Gelatin (which is a protein matrix holding a large percentage of water), we were able to easily observe very small deflections in the surface before the onset of wave motions. Measurements of the deflections indicated that they had the shape, scale and the frequency of occurrence of pockets, confirming our understanding that a pocket is a region of high pressure exerted on the wall under a turbulent boundary layer or channel flow by a convecting coherent motion. It is most often visualized as a region of aspect ratio order one, from which sublayer introduced marker has rapidly been moved.

6.3. Vorticity measurements using the photochromic technique

After several attempts to construct a static beam splitting device that will take a single laser beam and divide it into two sets of 10 beams that will cross to make a grid of 100 vorticity probes, we have succeeded

in producing a prototype, which has been specially silvered, and used to produce a rake of ultraviolet lines. When passed into kerosene doped with our photochromic chemical, we have obtained our first high resolution lines into a fluid. Using a pair of devices, we have produced grids with 100μm lines. An example of the original grid and its distortion after .4 seconds is shown in Figure 9. Using this vorticity probe, we plan to measure the vorticity in a Stokes layer created on our impulsively started moving belt to test the accuracy of the technique; then go on to measurement of transverse vorticity in a vortex ring; and then on to measurements of the streamwise vorticity in the streak produced by the vortex ring/wall interaction. In our ongoing study we are planning to measure the vorticity in the coherent motions in a turbulent boundary layer.

6.4. Modifications to the production process

Our knowledge of the elements of the production process has led us to examine how it changes in the presence of riblets in our simulation, and to determine how the presence of LEBU's affect the rate of production in a flow where the net drag has been lowered.

6.4.1. Vortex ring/moving plate interaction

Modifications that riblets can make to the turbulence production process are being studied to see what the most sensitive aspects of the process are. A 16 ft x 2 ft x 1.8 ft tank has been built which can use kerosene for future photochromic experiments, and has been outfitted with a moving plate that can be accelerated from rest to a constant speed. Using this facility, we first reproduced the interactions found using the moving

belt, and have recently started to examine the changes found when the vortex rings interact with the riblet covered wall. Our riblet surfaces are made by machining the desired geometry into a roller, and then impressing the riblets into sheets of wax. In this way, riblet plates can be made inexpensively, allowing us to investigate the effects of geometry on the interactions.

Our results using triangular riblets with spacing and height at the optimum as defined by Walsh 1982, i.e., h+ = 11, s+ = 22, showed that the riblets did not affect the formation of a long streak pair. On the contrary, the pair developed as usual with the exception that it was spaced 10% further apart. However, we observed that the pocket that was created was larger and seemed to be more pronounced. Interestingly, the presence of the riblets inhibited the appearance of secondary streaks under the same conditions that led to their formation and the ensuing catastrophic breakdown of the flow on a smooth plate. The conditions under which this evolution happens are fairly rare in a turbulent boundary layer, but stabilizing these occurrences might easily account for the observed 5% drag reduction in turbulent boundary layers. We must emphasize that only a small range of conditions has been investigated. Work is continuing to gain insight into the reasons riblets can shift this stability boundary.

6.4.2. Effects of LEBU's on the frequency of bursting

We have also investigated the effect of LEBU's on the frequency of occurrence of pockets at a position where the net drag was reduced by about 5%, but the local skin friction was reduced by approximately 40%. We found that the mean frequency of occurrence of the pockets decreased by 74% when

scaled on wall variables. Furthermore, the mean frequency also decreased when scaled on outer layer variables. This is consistent with our expectations.

An addtional fact emerged from these movies. There was less of an indication of the presence of the long streaky structure.

The above two facts, combined with two-point correlations and conditionally sampled measurements of the large eddy structure in the manipulated and normal layers (Rashidnia and Falco 1986) that indicate the decreased strength of the large scale structure, suggests that the large-scale wallward motions did not bring as many Typical eddies into close enough proximity with the wall. Thus, the number of Typical eddy/wall region interactions were reduced, and hence the skin friction.

7. THE VORTEX RING/VISCOUS WALL LAYER INTERACTION MODEL OF THE TURBULENCE PRODUCTION PROCESS

7.1. Introduction

Vortex ring-like microscale eddies which were found to exist across the turbulent boundary layer (Falco 1977, 1983) initiate the turbulence production process near walls through interaction with the wall region. An experimental simulation involving an artificially generated vortex ring interacting with a Stokes layer enables investigation of the interaction with reproducible initial conditions and in the absence of background turbulence. All of the observed features in the turbulent boundary layer production process such as the streaky structure, the pockets, the hairpin vortices, streak lift-up, oscillation, and breakup, have been observed to

form. The model shows us that hairpin vortices can pinchoff and reconnect, forming new vortex ring-like eddies.

Interestingly, the model includes interactions that occur with low probability in the turbulent boundary layer, but which contribute significantly to transport, and may be the events most readily controllable.

7.1.1. Discovery that vortex ring/wall interaction produces long streaks

As discussed above, we have discovered that over a certain range of parameters the vortex ring/moving wall interaction can produce long streaks. Only the lower speed rings can do this, and in our analogy, this means that only the higher speed Typical eddies of the boundary layer will produce a pair of long streaks before they create a pocket. There is an exception for high speed rings moving approximately parallel to the wall. As mentioned above, these observation have been made in the fully turbulent boundary layer. However, they were first observed in these simulation experiments.

Our observations in both the boundary layer and in the simulation experiments are admittedly incomplete, but we have a growing feeling that the streak spacing is primarily due to Typical eddies in the boundary layer. If it was not, and all other eddies contributed, there would be a uniform distribution of streaks resulting in essentially zero spacing, rather than the observed spacing of 100 wall layer units. In our proposed work, two different experiments are described to determine the answer.

7.1.2. Discovery that lifted hairpins 'pinch off' into vortex rings

Under a certain limited set of conditions -- shallow wallward angle and Ur > .6Uw --we have observed that the hairpin that lifts out of the pocket can undergo a rearrangement in which the legs come close together and diffusion processes take over, resulting in a vortex ring, with a new hairpin left behind. This is one mecha..ism for the regeneration process, in which new vortex ring-like Typical eddies can form in the turbulent boundary layer.

7.2. Vortex ring/moving wall interactions

7.2.1. Vortex ring interacting with a moving belt

We can simulate the interaction of a typical eddy with the wall region of a turbulent boundary layer by creating a vortex ring and having it convect towards a moving wall. Figure 10 shows the basic idea behind the simulation. The vortex ring can be aimed at or away from the wall at shallow angles. Both the wall and the ring move in the same direction. The Reynolds numbers based upon the initial ring velocity and diameter of the dyed ring bubble, D, range between 900 and 2000. When created away from walls, these rings remain stable to azimuthal instabilities over durations longer than those used in the interaction experiments. By performing a Galilean transformation on the simulation, we recover the essential aspects of the typical eddy wall region interaction in a turbulent boundary layer flow.

7.2.2. Evolutions of the model

We will describe the model in terms of the velocity ratios and spatial relationships of the simulation. Later in the discussion, we will invoke the Galilean transformation to relate the findings to the turbulent boundary layer case.

7.2.2.1. Fast rings (Ur/Uw > .45) moving towards the wall 3,6,9 degree

Interactions which result from these rings have been described by Liang, Falco and Bartholomew (1983). They result in the formation of a pocket, and varying degrees of lift-up of wall layer fluid. The interactions have been divided into four types. Figure 11 shows sketches of the four types of interaction. Type I results in a minor rearrangement of the wall layer fluid followed by the ring moving away from the wall essentially undisturbed. Type II (same as described for boundary layer interactions) results in a well defined lift-up of wall layer fluid, which takes on a hairpin configuration. This fluid does not get ingested into the ring, and the ring moves away from the wall perturbed, but still a stable ring. The hairpin has been observed to pinch-off, or just move back down towards the wall and dissipate. Type III (also described in section 3.4) results in a lifted hairpin of wall layer fluid which gets ingested into the ring, resulting in a chaotic breakdown of both the lifted hairpin and the vortex ring, as the vortex ring is moving away from the wall. Type IV also initiates a hairpin vortex, but in this case the hairpin vortex is ingested into the ring on a much shorter timescale, and the ring and lifted wall layer fluid both breakdown while the ring is very close to the wall.

Further research needs to be done. Liang et al(1983) used vortex rings with $D^+ > 250$ and $\delta+$ between 20 and 50, and they observed only the above four types of interactions. Our experiments indicate that if $D^+ < 150$ and $\delta+$ is between 20 and 50, we can also obtain the four types of interactions noted above, but, in addition, we found that long streaks also formed. In these cases, a hairpin grew out of the open end of the pocket, its legs stretched and a pair of streamwise streaks formed along side the hairpin legs. The streaks grew to several hundred wall units. This observation is in contrast to the suggestions of a number of investigators that a lifted hairpin vortex would induce a single streak to form between its legs.

7.2.2.2. Slow rings (Ur/Uw < .35) moving towards the wall at a shallow angle 3,6,9 degrees

These initial conditions result in a pair of long low speed streaks, $x^+ = O(1000)$, a pocket, and hairpins which induce themselves and portions of the streaks to lift-up. Figure 12 shows six photos of this happening prior to the onset of a Type III interaction. We can see the formation of the pair of low speed streaks, followed by the formation of the pocket, and the associated hairpin lift-up, then partial ingestion of the pocket hairpin. The ring later breaks up. The streaks that form under these conditions become wavy and slowly breakdown resulting in additional lift-up and transport. Hairpins have been observed to form over these streaks. The initial conditions are two-dimensional. The moving belt is started from rest, so that the layer approximates a Stokes layer. These streaks have obviously not formed as the result of the pre-existence of streamwise vortices, but spanwise vorticity has been distorted to give a streamwise

component, and it is clear from the Navier Stokes equations that new streamwise vorticity has also been generated at the wall.

7.2.2.3. Fast rings (Ur/Uw > .45) moving away from the wall at a shallow angle (less than 3 degrees)

These initial conditions result in a hairpin vortex which is linked to the distributed streamwise vorticity that has formed a pair of long, very stable, low speed streaks. A pocket is not observed. The evolution of the hairpin in this case has been observed to lead to the pinch-off of this hairpin, forming a vortex ring, and another hairpin. Figure 13 shows four photos of the evolution leading to the creation of a new vortex ring. The long stable streaks which form, come closer and closer together, indicating that the streamwise vorticity which caused them, and which is of opposite sign, is being stretched and brought very close together. Diffusion is accelerated, and the vorticity is redistributed into a vortex ring and a hairpin loop. Figure 14 shows long very stable streaks and a long stretched hairpin which does not pinch-off over the distance available due to size limitations of the experimental facility--more than 2500 wall layer units. There are two initial conditions that may cause this kind of long stretched streamwise vorticity to evolve into a hairpin: 1) δ/D is very small; 2) the ring is far away from the wall. Further study concerning the effects of ring to wall distance is needed.

7.2.2.4. Slow rings (Ur/Uw < .45) moving away from the wall at a shallow angle

These initial conditions result in a hairpin from which a pair of long stable low speed streaks emerge. A pocket is also not observed. It is possible that the process may be an important part of the turbulence regeneration mechanism, but not directly a part of the bursting process, because it doesn't contribute much uv. The phenomena of hairpin pinch-off, for this case, appears to depend upon δ/D. If $\delta/D < .15$, we get pinch-off, but only a part of the fluid involved in the hairpin is observed to pinch-off and form the ring. If δ/D is greater and the ring moves away from the wall without ingesting any wall layer fluid (Type I or II), the lifted hairpin appears to do very little. Figure 15 shows four photos of the evolution for $\delta/D > .15$. In this case a pocket does not form, and it appears that the hairpin has been generated by the initial vortex ring/wall interaction, and that a pair of streamwise vortices--which could be called its legs--trail behind, creating the streak pair. Pinch-off does not occur. Figure 16 shows four photos of the interaction for $\delta/D < .15$. In this case, pinch-off of a portion of the lifted hairpin does occur, creating a new small vortex ring.

7.2.2.5. Summary of interactions

A summary of the vortex ring/wall interactions which result in streak formation and evolution is shown as a function of the parameters Ur/Uw, δ/D, and ring angle in Figures 17 and 18. Figure 17 shows the dependence of the formations and evolutions of streaks on δ/D and Ur/Uw for $D^+ > 250$ and a 3 degree incidence angle. The indicated boundaries are between different

evolutions and are approximate additional data is necessary to precisely locate their positions. The information available suggests that the streak development is essentially independent of δ/D. Furthermore, the long streaks are only observed to form for speed ratios less than approximately .45. Figure 18 shows the dependence of δ/D on Ur/Uw for rings moving away from the wall at 2.5 degrees. δ/D now plays a much more important role, and long streaks are generated over the entire speed ratio range studied.

7.2.3. Scaling associated with the vortex ring/moving wall interactions

From our perspective of a turbulence production model, the streak spacing, streak length and wavelength of the streak instability are quantities of interest.

7.2.3.1. Streak spacing

Figure 19 shows the dependence of the streak spacing in wall units on the size of the vortex ring in wall units, for an incidence angle of 3 degrees and Ur/Uw = .31. The thickness of the wall layer (in wall units) is shown next to each data point. The streak spacing, z^+, is within 10% of the ring diameter for wall layer thicknesses between 20 and 50 wall units. Results shows that decreasing Ur/Uw will decrease the average streak spacing relative to the ring size for fixed incidence angles. Furthermore, increasing the incidence angle of the vortex ring will increase the average streak spacing for a given ring size and speed ratio. Figure 20 shows the dependence of the streak spacing on the speed ratio and angle.

7.2.3.2. Streak length

Measurements show that streak lengths greater than $x^+ = 500$ were obtained for many of the interactions in ranges where the streaks are stable (for rings with $D^+ = 100$, streaks as long as $x^+ = 1000$ were found).

7.2.3.3. Wavelength associated with wavy streak instability

Figure 21 shows the non-dimensionalized streamwise wavelength that sets in as a function of δ^+ for different Ur/Uw. The wavelength is the same order as the ring diameter. It decreases as the ring/wall speed ratio decreases.

7.2.4. Stability considerations

7.2.4.1. Vortex ring stability

Some additional data has been obtained, which confirms and extends the results of Liang (1984), showing the boundary between stable ring wall interactions (Types I and II), and unstable interactions (Types III and IV) depends upon δ/D. Figure 22 shows a stability map of the interactions for 3 degree rings. We can see that for low ring/wall speed ratios, the ring stability depends primarily upon the relative thickness of the wall layer and the size of the ring for thicker wall layers, or smaller rings the interactions are more stable. Furthermore, the shallower the incidence angle the more stable the interaction.

7.2.4.2. Stability of the streaks

We spent considerable time deciding upon a measure of the time to instability of the streaks which exhibited wavy instability.Figure 23 shows

the dependence of the time to instability of the streaks which exhibited wavy instability on the wall layer thickness (both quantities non-dimensionalized by wall layer variables) for 3 degree incidence rings. We can see that for each convection velocity ratio, there is a value of δ^+ above which the time to instability becomes much longer. As the ring/wall speed ratio increases, the critical thickness of the wall layer needed to increase the time to instability decreases.

7.2.4.3. Comparison between ring and streak stability

Both the rings and the streaks are more stable when the wall layer is thicker. Figure 22 shows a comparison of the stability boundaries of a three degree ring moving towards the wall, and of the boundaries of stable streak formation those rings can create. It turns out that both the ring stability boundaries (and the streak stability boundaries) for different size rings collapse when plotted this way.

The streak formation boundaries in this figure represent the boundaries between conditions that will enable a pair of long streaks to form. For δ/D below the boundaries, we have a very unstable situation in which the fluid in the region around the eddy seems to rearrange itself into the beginnings of a streak, but the streak pair is not stable, and immediately breaks up. For δ/D values above the boundaries, a pair of long streamwise streaks form. However, once formed, the streaks are susceptible to breakdown by the wavy or lumpy instabilities noted above, where the time to instability is a function of angle, convection velocity, and the instantaneous wall layer thickness (for example, see figure 23).

7.3. Implications for turbulent boundary layers

7.3.1. Connection between vortex ring/wall layer description and the typical eddy wall layer interaction

To interpret the results of the vortex ring/moving wall interactions in terms of turbulent boundary layer interactions, we must perform a Galilean transformation on the velocity field. Our interpretation of the simulation has been to identify the Stokes layer with the viscous wall region which extends to y^+ approximately 30-50. The mean velocity at this height is approximately 70 -80% of U_∞. Thus,

$$U_{TE}/U_\infty = a(1 - Ur/Uw)$$

where 'a' represents the outer region velocity defect which we cannot simulate (20-30%), and U_{TE} is the convection velocity of the Typical eddy. Thus, in thinking about the implications for the turbulent boundary layer, basically high speed ratios in the simulations correspond to low convection velocities of the typical eddies in the boundary layer.

As a result, we expect the typical eddies that emerge from wall layer fluid (through a pinch-off of lifted hairpin vortices, for example) to have a low convection velocity. Since these are moving away from the wall, they will correspond to fast rings moving away from the wall. These exhibit long streak formation which is stable, and pinch-off, depending upon the thickness of the wall layer. We do see long stable low speed streaks in the boundary layer, and we have limited evidence of hairpin pinch-off. On the other hand, typical eddies that are convecting towards the wall will be of relatively high speed, and thus simulated by low speed vortex rings moving

towards the wall. These will produce long streaks which go unstable (undergoing either wavy or lumpy instabilities), short streaks which go unstable, and pockets in all cases. Again we see all these events in the turbulent boundary layer.

The wide range of interactions that can be simulated using the vortex ring/moving wall experiments are not all admitted by the turbulent boundary layer with equal frequency. Some are not admitted at all. The range of the parameters (angle, wall layer thickness, convection velocity) found in the boundary layer are limited, and in all cases they have skewed probability distributions (towards higher values) that are approximately lognormal. When these distributions are used to determine the events that are most probable, we begin to see what to expect.

Figure 24 shows the distribution of D^+ obtained from the diameter of the typical eddies of a turbulent boundary layer at $R_\theta = 1176$, superimposed upon the streak spacing obtained for various size rings. When the simulation outcomes are conditioned by the probabilities of scales found in this boundary layer, we see that the simulation gives a most likely streak spacing of approximately 100 wall units. This is an important quantitative test of the quality of the simulation, for although the average streak spacing is $\lambda^+ = 100$, all observations of streak pairs have also shown their spacing to be approximately this value.

We have very limited information about distributions of this type for the angles of incidence and/or movement away from the wall, for the convection velocity, and for the instantaneous wall layer thickness, but the evidence indicates that the frequency of occurrence of many of the interactions which we can simulate is quite low in the turbulent boundary

layer. Often these interactions are very intense. Thus, the conditions in the boundary layer that exist which keep their probability low are likely to be essential to the maintenance the measured values of the drag. We need to explore ways to further limit the occurrence of the violent breakups if we are to pursue a rational program of drag reduction (and noise reduction) in the boundary layer. The model allows us to isolate a specific high drag producing event, and carefully study the parameters that it depends upon. We are currently building the sample sizes necessary to more accurately obtain the distributions mentioned above.

7.3.2. Implications for drag modifications

As we have seen, small changes in the parameters of typical eddy size, incidence angle, convection velocity, and wall layer thickness can alter the evolutions that result when a typical eddy interacts with the wall. Changes in any of these variables which cause a cross over in the boundaries (such as those shown in Figures 17 and 18), will result in a change in the drag at the wall.

Consider, for example, the angle of incidence. If we can change the strength of the large scale motions, say, by outer layer manipulators, we can easily change the angle of a typical eddy that is moving towards the wall, and may even be able to change the direction if it is at a shallow angle, so as to make it move away from the wall. This will effect the stability of both the local eddy wall interaction (interactions of Type I-IV), and the stability of the streaky structure which is created, as well as the formation of new typical eddies via the pinch-off process. Thus, we

can affect not only the local drag, but alter the drag downstream by directly interfering with the cyclic production process.

Modifications to the wall that result in small changes in the effective wall region thickness, for example NASA riblets, will also have an effect on the drag. If increases in wall region thickness above the critical thicknesses can be made (see for example, Figures 18 and 22), streaks are more likely to remain stable. Furthermore, the local interactions (Types I-IV) will also tend to be of Type I and II. Thus, the drag can also be reduced. Streaks will, under these circumstances, undergo disturbances from ambient turbulence before self instability.

Finally, changes in the wall geometry (for example, the riblet configurations), can change the underlying production of vorticity, which may result in changes in the classifications, as well as the positions of the boundaries, of the stability maps (see discussion in section 6.4.1).

7.4. Conclusions

New findings in the turbulent boundary layer have suggested that long low speed streaks are formed in pairs as the result of the interactions of microscale very coherent vortex ring-like eddies (typical eddies) propagating over the wall. Depending upon the distance from the wall, the angle of incidence of the eddy with the wall (both magnitude and sign), the convection velocity of the eddy, and the local thickness of the viscous wall region, different structural features can evolve out of the evolution. The extent of the distance over which a typical eddy could interact with the wall and wall layer flow was a surprise, but means that many coherent

microscale eddies that are in the logarithmic region and further out take part in the production process.

The vortex ring/moving wall simulation incorporates all of the evolutions and structural features associated with the turbulence production process. It dramatically demonstrates that streamwise vortices are not required to produce streamwise streaks. When the streak spacings obtained in the simulation are conditioned by the probability of occurrence of typical eddy scales found in the boundary layer, we see that the simulation provides the correct streak spacing (approximately 100 wall units). Other possible outcomes of the simulation need to be weighed by the measured probabilities of occurrence of the angles, convection velocities, and length scales of the typical eddies in the turbulent boundary layer to enable us to obtain a picture of the most probable forms of the interactions, and to gain insight into the causes of the interactions which occur with lower probability, that may contribute significantly to the transport. It appears that turbulent boundary layer control leading to drag reduction can be realized by fostering the conditions suggested by the simulations which will increase the probability of having stable interactions.

8. SOME QUESTIONS THAT REMAIN TO BE ANSWERED

We have now seen that the passage of a vortex ring over a Stokes layer results in all of the structural features associated with the bursting process. Furthermore, the Typical eddy is closely modeled by a vortex ring. Thus, it would appear that we have the sought after understanding of the mechanism of turbulence production. However, although

we have the agent, and the morphology, we do not understand the detailed mechanisms of each step of the process, and thus, do not have the knowledge to intercept the chain of events, to affect the outcome we would like. Of course, to be able to make the statement that a) there is a chain of events, and b) that we know the overall cause, is our major result. But the detailed causal reasons behind each of the steps in the process are necessary goals of further research. We try to highlight some of the unknowns in the following discussion.

8.2. Creation of streamwise vorticity and streaks from outer region motions

An important question is whether the creation of the long streaks is primarily an integral pressure effect due to the passage of the eddy over the wall, i.e., another way to ask this is whether the shape of the Typical eddy is important, vs. just its size and normal velocity component. The Navier-Stokes equations provide some guidance. Taken to the limit in the near wall region they indicate that

$$\partial p/\partial z = \nu \partial \omega_x/\partial y$$

for example, so that streamwise vorticity is created if any arbitrary instantaneous pressure gradient is created. Obviously if the integral over a given area is larger, we will see more vorticity, thus the equation indicates that the distribution of pressure is important. The coherence of the Typical eddy pressure pulse is thus a parameter that is of importance in the boundary layer responding to it by creating streaks. However, we do not know what the limits are beyond which the pressure gradient is too weak to create streaks.

It is interesting to note that although we are thinking about a smooth wall, the same statement applies to a wall of any shape. Thus, for example, the presence of riblets may significantly alter limits, shifting them so as to reduce the number of Typical eddies capable of creating streaks.

8.2.1. Importance of the internal dynamics of the excitation eddy

A more subtle possibility is that the Typical eddy's internal dynamics is important. This would relate directly to the formation of the primary hairpin vortex (that is associated with the pocket in cases where the Typical eddy is moving towards the wall). It is certainly true that the vortex ring will induce fluid up from the wall, and thus, if the Typical eddy is moving faster than the wall region flow, a hairpin will result that is stretched.

8.3. What has created the long streaks?

Because we are unsure of the relative role played by the Typical eddy, i.e., overall pressure gradient or primarily effect of internal dynamics, or, most probably, some combination of the two, we cannot isolate the primary causal factor in the formation of the long streaks. In our three view results obtained from the simulations, we cannot see any evidence of streamwise vortices (there is almost certainly streamwise vorticity) in the region where the streaks first form. In these experiments (still in progress) we have a fixed laser sheet that gives us the cross-stream view, as the event passed through it. As time progresses we observe the streaks pass through the laser sheet, then, after some significant

length of streak has passed, we see our first evidence of vortices. They appear as a flattened pair of counter-rotating vortices surrounding each streak. As more of the interaction region passes through the laser sheet, the pair soon become round and lift themselves away from the wall, lifting the streak with them. The diameter of these vortices is proportional to the width of the streak, not to the spacing between streaks. This is different from the picture drawn dozens of times in the literature of a pair of counter-rotating vortices spanning the gap between the two streaks. Figure 25 illustrates the differences. There is an apparent roll-up of streamwise vorticity into streamwise vortices. However, it is not at all clear how a pair of streamwise vortices formed. Irrespective of whether the primary hairpin or the overall pressure was responsible for the initiation of the long streaks, they both would result in streamwise vorticity of only <u>one</u> sign. Thus another set of questions arises.

8.3.1. What creates the vorticity of opposite sign?

The creation of the vorticity of the opposite sign can be due to a response of the wall layer to the sign of the initial streamwise vorticity. This would be a viscous effect, and would be the direct consequence of the no slip condition.

The other possibility arises as a possible consequence of the following observation. As the moving wall convects more of the interaction through the laser sheet, we move closer to the pocket and find that these pairs of counter-rotating vortices boardering the streaks are actually the legs of hairpins. Moving up past the location of the pocket, we move out of the pair and into another pair of counterrotating vortices and through a

second hairpin head. Thus, it is possible that the hairpins formed because the streak closer to the pocket is stronger, and that they stretched, amplified, and their legs appeared as the pair, which eventually lifted up the streak. However, each streak of the pair existed before these hairpins could form.

If the legs of the primary hairpin vortex are the main contributor to the streaky structure, the mechanism would still be different from the currently proposed picture of how it is done. It is currently argued that a streak would form between the legs of a hairpin. In our experiments we find that both streaks form in between the primary hairpin vortices' legs.

Thus, the details of how a Typical eddy ultimately creates the long streaks is not clear. It is entirely possible that the viscous image of the rolled up vorticity forms, and it and the original vortex combine with a Kelvin Helmholtz instability of the strong defect regions of each long streak reconnecting to form the hairpins. This may in fact be the mechanism of all observed hairpins that straddle streaks.

Some answers to these questions will come when we convert our apparatus from one where the event is evolving as the belt carries the events through the fixed laser sheet, one where we can keep the laser sheet at a fixed location in the event to determine what goes on at a fixed position with increasing time. This is currently being done.

We see streaks long before we see hairpins, so it appears that hairpins are not necessary to create streaks. But, we now understand how boundary layer investigators have made the interpretations they have. The lifted portions of these streaks seem to be associated with hairpins, a conclusion first suggested by Kline et al (1967). However, this statement

is not sufficient to suggest that we understand even this limited aspect of the turbulence production process near walls.

8.3.2. Occasions when long streaks are created but not hairpins.

When the vortex ring is moving away from the wall, a very stable pair of streamwise vortices is formed, which gather up marker into their cores so that a long streak pair appears. The legs of the hairpin have the same sign as the long swath of streamwise vorticity, so in the overlap region, they merge, pair, or coalesce, and we get the impression of a hairpin vortex with very long legs. These vortices/streaks are very stable and we do not observe the formation of hairpins with respect to them.

8.3.3. Further information on the interaction of the primary hairpin and the pressure gradient created streamwise vorticity

For a large majority of the time, the Typical eddy is of type 1 or 2; in these cases, it does not ingest the lifted hairpin vortex. The hairpin remains coherent for a long enough development time to have its legs get stretched significantly. These legs, which of course terminate at the wall, overlap the long streamwise vortices produced by the same ring, which, of course, also terminate at the wall. The sign of the vorticity in the streamwise streaks has the <u>same</u> sign as the vorticity in the legs of the hairpin vortex. Thus, in the region where they both exist they can coalesce or merge. Under a number of conditions as $Ur/Uw > .35$, we have observed that the legs of the hairpin tend to be spread further apart than the pair of long streamwise vortices. These legs form a second pair of streaks outside of the primary pair.

8.3.3.1. Evolution as seen in end-view laser sheet for Ur/Uw < .35

Continuing our description of the evolution of the bursting process, as the flow moves through the laser sheet to the position of the pocket, we see a rapid movement to the center line of the event, i.e., rotation towards the centerline of the pocket. The cross-stream wall vorticity, which has been distorted during the pocket formation, and which forms the pocket vortices, has by this time been significantly stretched. It is this amplified vorticity that induces the streamwise vortex pair (and its hairpin head) towards the center of the pocket. In doing this, the hairpins are strongly distorted, and the lifted portion of the streaks between them appear to breakup.

8.3.4. Spot formation

As we increase the velocity ratio above .35 we begin to see what appears to be a repeat of the process with a third pair of streaks forming, and perhaps additional pairs. The overall visual impression is that a turbulent spot has formed. Experiments show that as Ur/Uw increases to, say, .5 from .35, we get a more vigorous spot. It is not clear why this happens. It does, however, warn us that simulations must be performed and studied in their range of validity.

8.4. Implications for control of boundary layer turbulence

If we hypothesize that Typical eddies are the major causative factor in the creation of both the long streaks and the pockets, and if the breakup of the long streaks and the liftup of the fluid in the pocket and

its ingestion into the ring and ring breakdown are the major causes of turbulence energy production, we have the basis for a number of controls on the turbulence energy production process. The effectiveness of the controls suggested by the vortex ring/wall experiments depends upon a) whether the distribution of vorticity in the Typical eddies is similar to that in the artificially generated vortex rings, b) whether the distribution of vorticity in the Stokes layer is similar to that in the sublayer, and c) whether the sensitivity of the vortex rings/Stokes layer interaction to changes in δ/D, Ur/Uw, and angle of incidence, is similar to the sensitivity of the Typical eddy/sublayer interaction. We present results below of our ongoing study of these sensitivities in the simulations.

8.4.1. Example of controls to reduce drag

Figure 22 shows the streak/ring stability situation with the abscissa also indicating the situation as it would appear in the boundary layer. It is for a constant angle of incidence. The lines on the map indicate the stability boundaries, which are quite sharp. This is true for both the ring and the streak stability boundaries. If the boundaries are as sharp in the turbulent boundary layer, we will have important opportunities for control. For example, by changing the eddy size, or the sublayer thickness, or the angle of incidence (weakening the large eddies) by a very small amount, we can move an eddy that is at a point on the unstable side of either the streak or the eddy stability boundary, or both, across the stability boundaries to make its interactions stable. Other ideas involve learning how to: a) reduce the frequency of the Typical eddies--by inhibiting their formation or by causing them to dissipate faster; b) prevent the Typical

eddies from getting close enough to the wall to interact; c) thicken the wall layer so that the interactions are weakened; and d) change the vorticity distribution within the eddies so that the stability maps change, shifting to more stable positions. Many others come to mind, but until we determine the sensitivity to the parameters, the most efficient path to control will not be clear.

9. OVERALL CONCLUSIONS

Research into the mechanism of turbulence production has shown that a single outer region coherent motion interacts with the wall to initiate the process. Then a cascade of events is set in motion, in which streaks form, pockets form, hairpins form; then streaks are lifted up, hairpins are lifted up, and some pinchoff and reconnect to form new Typical eddies. Although any scale of pressure perturbation can in principal initiate the process, it appears that the Typical eddy is most often the cause. Why this is so is not clear. The reason for the dominance of some competing mechanisms that take over once the process is initiated is also not completely understood. It is shown in simulation experiments that certain overall parameters are involved. Work is proceeding to determine the role played by these parameters.

10. Acknowledgements

It is my pleasure to acknowledge the major contribution that my students C. C. Chu, J. Klewicki and J. Chang have made in obtaining the underlying data for this report. This research was sponsored by the Air Force Office of Scientific Research under Contract No. F49620-85-C-0002. We

would like to thank Dr. Jim McMichael for his encouragement and advice as contract monitor.

11. References

Acarlar, M.S. and Smith, C.R. 1984: An experimental study of hairpin-type vortices as a potential flow structure of turbulent boundary layers. Rept. FM-5, Dept. of M.E./Mech., Lehigh Univ.

Andreopoulos, J., Durst, F., Jovanovic, J. and Zaric, Z. 1984: Influence of Reynolds number on characteristics of turbulent wall boundary layers.

Balint, J.L., Vukoslavcevic, P. and Wallace, J.M. 1986: A study of the vortical structure of the turbulent boundary layer. Proceedings of the European Turbulence Conference, Lyon, France, July 1-4.

Blackwelder, R.F. and Kaplan, R.E. 1976: Burst detection in turbulent boundary layers. J. Fluid Mech. 76, pp. 89-101.

Falco, R.E. 1974: Some comments on turbulent boundary layer structure inferred from the movements of a passive contaminant. AIAA Paper 74-99.

Falco, R.E. 1977: Coherent motions in the outer region of turbulent boundary layers. Phys. Fluids Suppl. II 20, S124-S132.

Falco, R.E. 1978: The role of outer flow coherent motions in the production of turbulence near a wall. in Coherent Structure of Turbulent Boundary Layers ed. C.R. Smith and D.E. Abbott pp. 448-461.

Falco, R.E. 1980a: The production of turbulence near a wall. AIAA Paper No. 80-1356.

Falco, R.E. 1980b: Structural aspects of turbulence in boundary layer flows. in "Turbulence in Liquids" ed. Patterson and Zakin, pp. 1-15.

Falco, R.E. 1980c: Combined simultaneous flow visualization/hot-wire anemometry for the study of turbulent flows. J. of Fluids Engr. 102, pp. 174-183.

Falco, R.E. 1982: A synthesis and model of wall region turbulence structure. In "The Structure of Turbulence, Heat an Mass Transfer" ed. by Z. Zoric', pp. 124-135, Hemisphere Press.

Falco, R.E. 1983: New results, a review and synthesis of the mechanism of turbulence production in boundary layers and its modification. AIAA Paper No. 83-0377.

Foss, J.F., Klewicki, C.L. and Disimile P.J. 1986: Transverse vorticity measurements using an array of four hot-wire probes. NASA CR 178098.

Head, M.R. and Bandyopadhyay, P. 1981: New aspects of turbulent boundary layer structure. J. Fluid Mech. 107, pp. 297-337.

Kim, J. 1986: Investigation of turbulent shear flows by numerical simulation. Tenth Congress of Applied Mechanics, Austin TX, June 16-20.

Kim, J., Moin, P. and Moser, R. 1986: Turbulence statistics in fully developed channel flow. Submitted to J. Fluid Mech.

Klewicki, J. and Falco, R.E. 1986: Spanwise vorticity distributions and correlations in a turbulent boundary layer. Bull. Am Phy. Soc. 31, 1685.

Kline, S.J., Reynolds, W.C., Schraub, F.A. and Runstadler, P.W. 1967: J. Fluid Mech. 30, 741

Kim, H.T., Kline, S.J. and Reynolds, W.C. 1971: The production of turbulence near a smooth wall in a turbulent boundary layer. J. Fluid Mech., 50, 133.

Liang, S. 1984: Experimental investigation of vortex ring/moving wall interactions. MS Thesis, Dept. Mech. Engr. Michigan State Univ.

Liang, S., Falco, R.E. and Bartholomew, R.W. 1983: Vortex ring/moving wall interactions: experiments and numerical modeling. Bull. Am. Phy. Soc., Series II, 28, p. 1397.

Lovett, J. 1982: The flow fields responsible for the generation of turbulence near the wall in turbulent shear flows. MS. Thesis, Dept. Mech. Engr. Michigan State Univ.

Moin, P., Leonard, A. and Kim, J. 1986: Evolution of a curved vortex filament into a vortex ring. Phy. Fluids 29, pp.955-963.

Oldaker, D.K. and Tiederman, W.G. 1977: Spatial structure of the viscous sublayer in drag reducing channel flow. Phy. Fluids 20 (10), pp. 133-44.

Praturi, A.K. and Brodkey, R.S. 1978: A stereoscopic visual study of coherent structures in turbulent shear flow. J. Fluid Mech. 89, pp. 251-272.

Runstadler, P.W., Kline, S.J. and Reynolds, W.C. 1963: An experimental investigation of the flow structure of the turbulent boundary layer. Dept. of Mech. Engr. Rep. MD-8, Stanford Univ.

Schraub, F.A. and Kline, S.J. 1965: Study of the structure of the turbulent boundary layer with and without longitudinal pressure gradients. Dept. of Mech. Engr. Rep. MD-12, Stanford Univ.

Smith, C.R. 1982: Application of high speed videography for study of complex, three-dimensional water flows. SPIE 348, "High Speed Photography" (San Diego), pp. 345-352.

Smith, C.R. and Metzler, S.P. 1983: The characteristics of low-speed streaks in the near-wall region of a turbulent boundary layer. J. Fluid Mech. 129, p. 27.

Walsh, M. 1982: Turbulent boundary layer drag reduction using riblets. Presented at the 12th AIAA Aerospace Sciences Meeting.

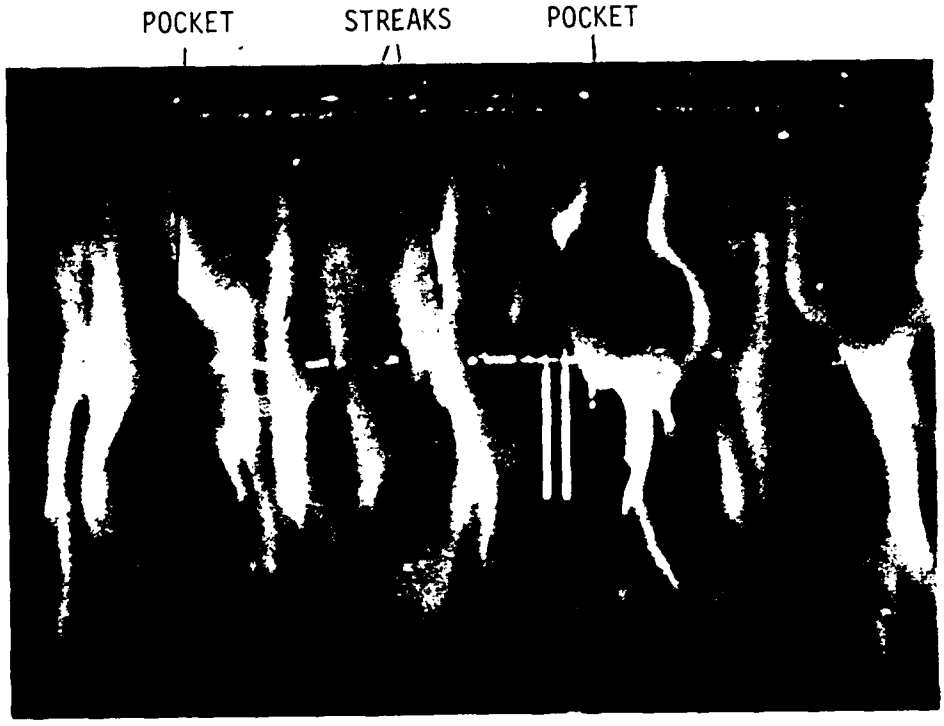

Fig. 1. Two pockets and a pair of streaks as seen in wall slit visualization of the sublayer of a turbulent boundary layer using smoke as the contaminant in air. The slit is at the top of the photo, and the flow is from top to bottom.

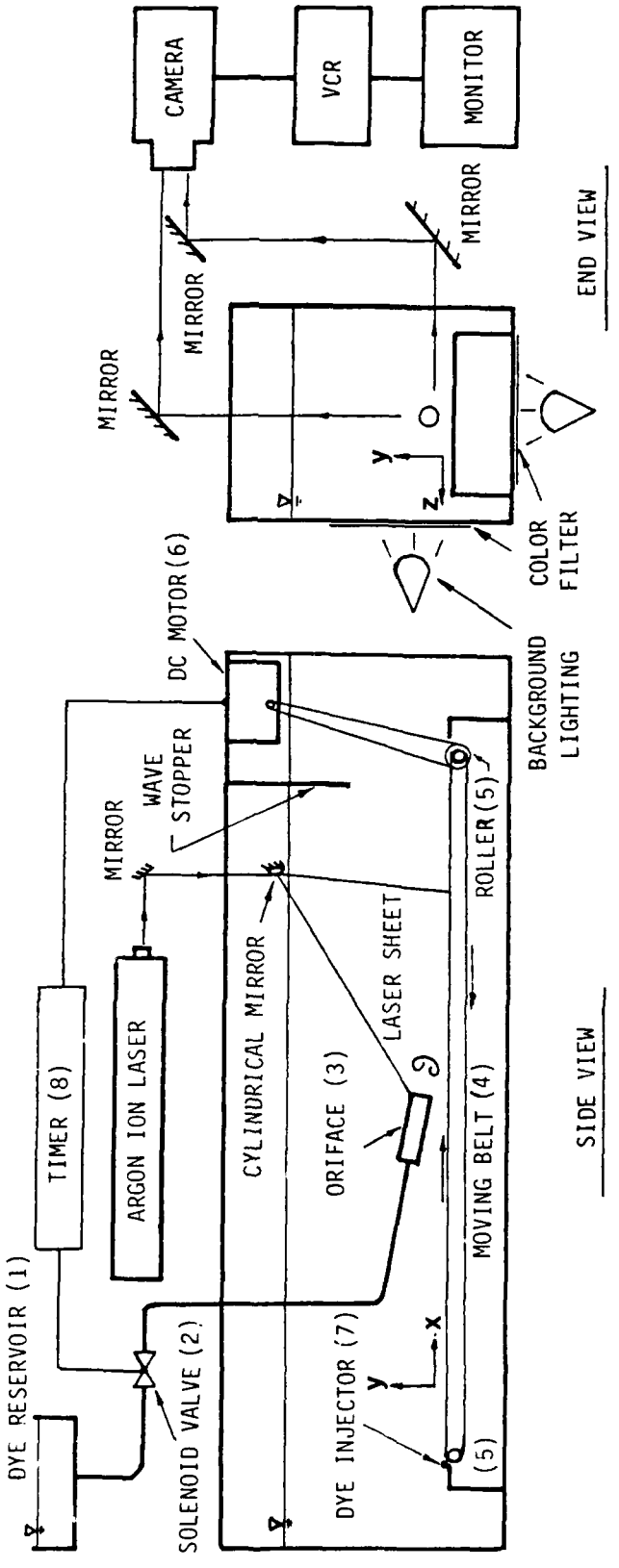

Fig. 2. Side and end views of a schematic of the experimental apparatus used in the vortex ring/moving wall simulations.

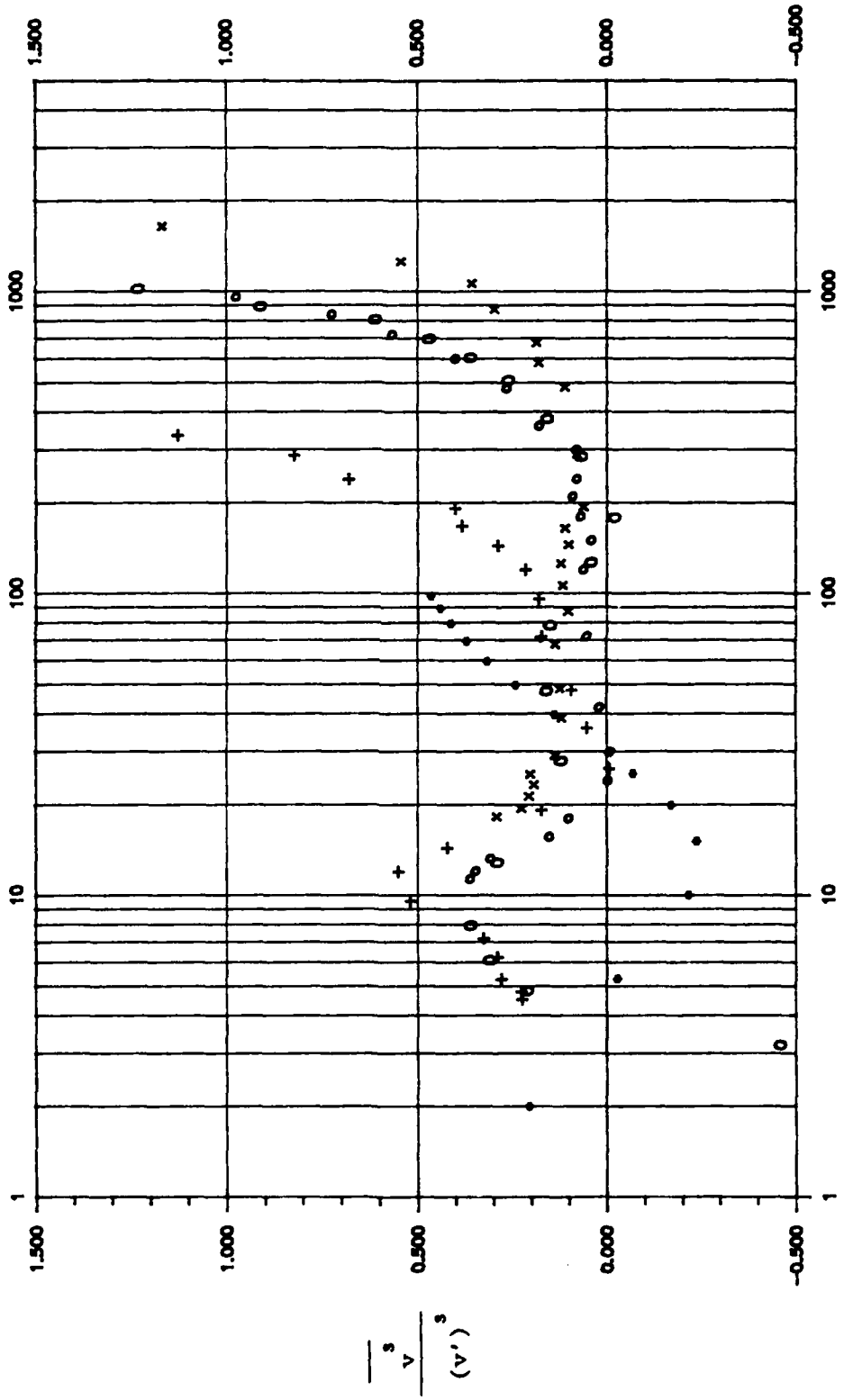

Figure 3. The Skewness of the normal fluctuations, v. O are data of Andreopoulos et. al., (1984); * are computations of Kim et. al. (1986).

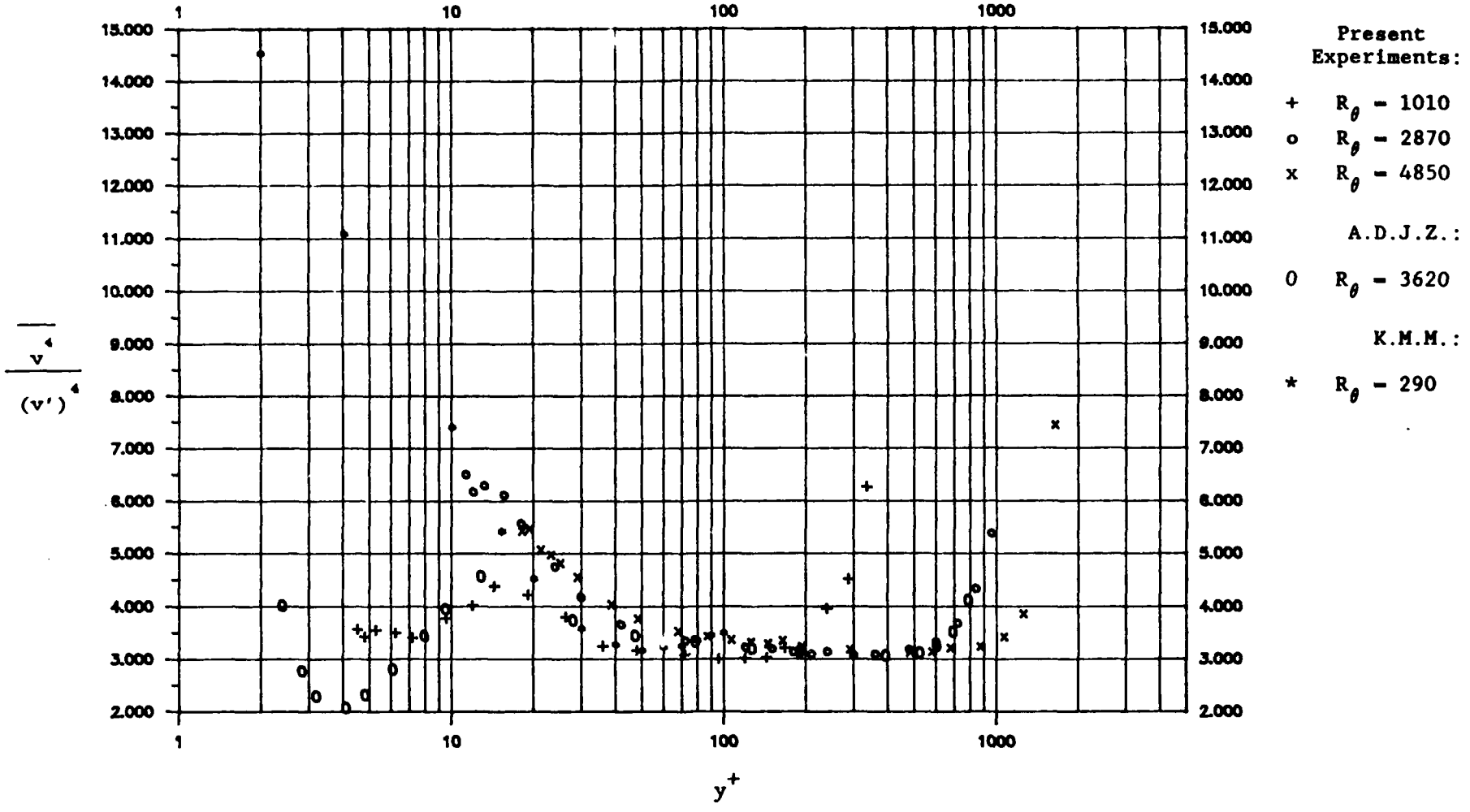

Figure 4. The Flatness of the normal velocity fluctuations, v. O are data of Andreopoulos et. al., (1984); * are computations of Kim et. al. (1986).

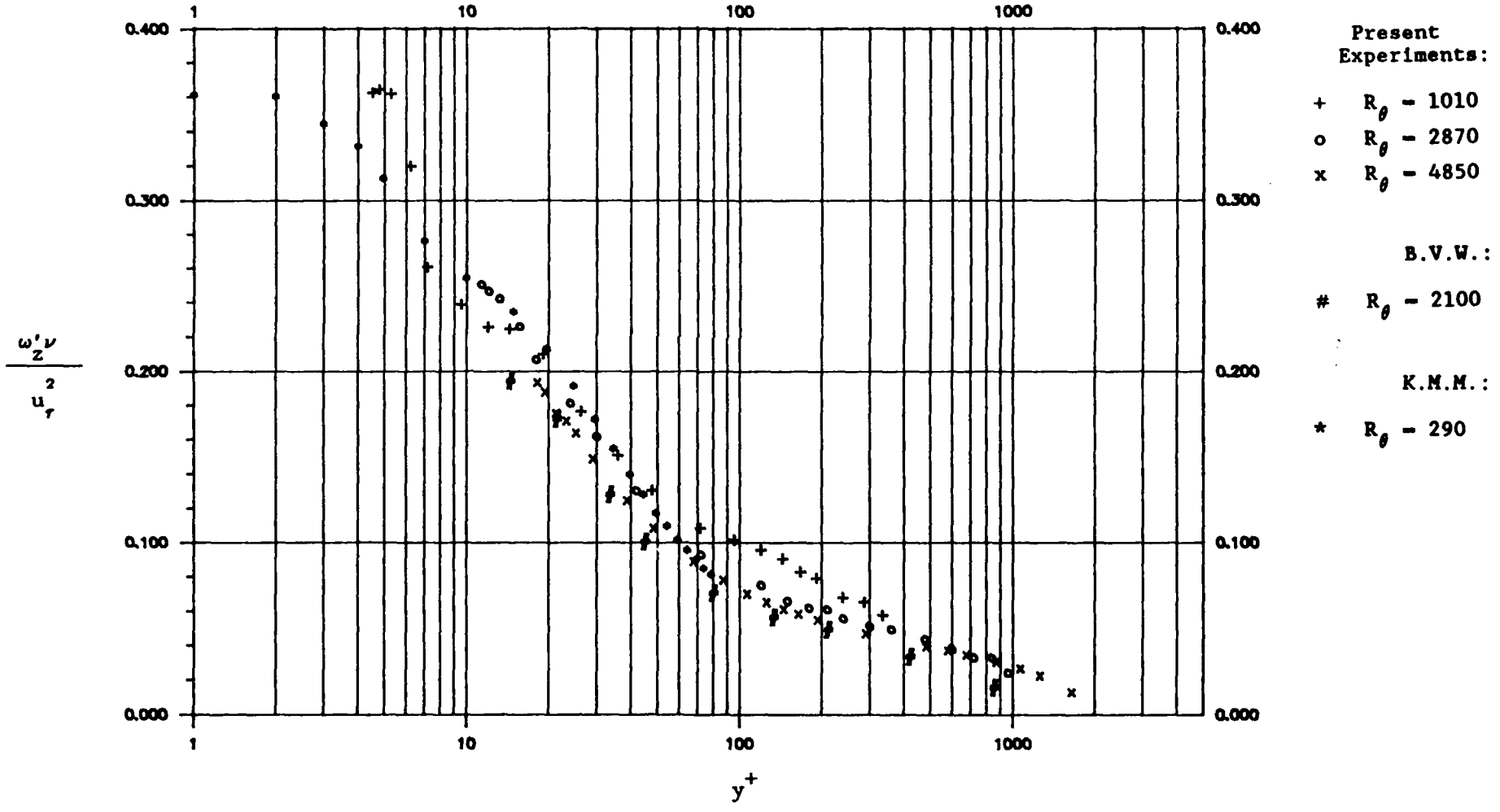

Figure 5. The rms ω_z normalized by wall variables. # are data of Balint et. al. (1986); * are computations of Kim et. al. (1986).

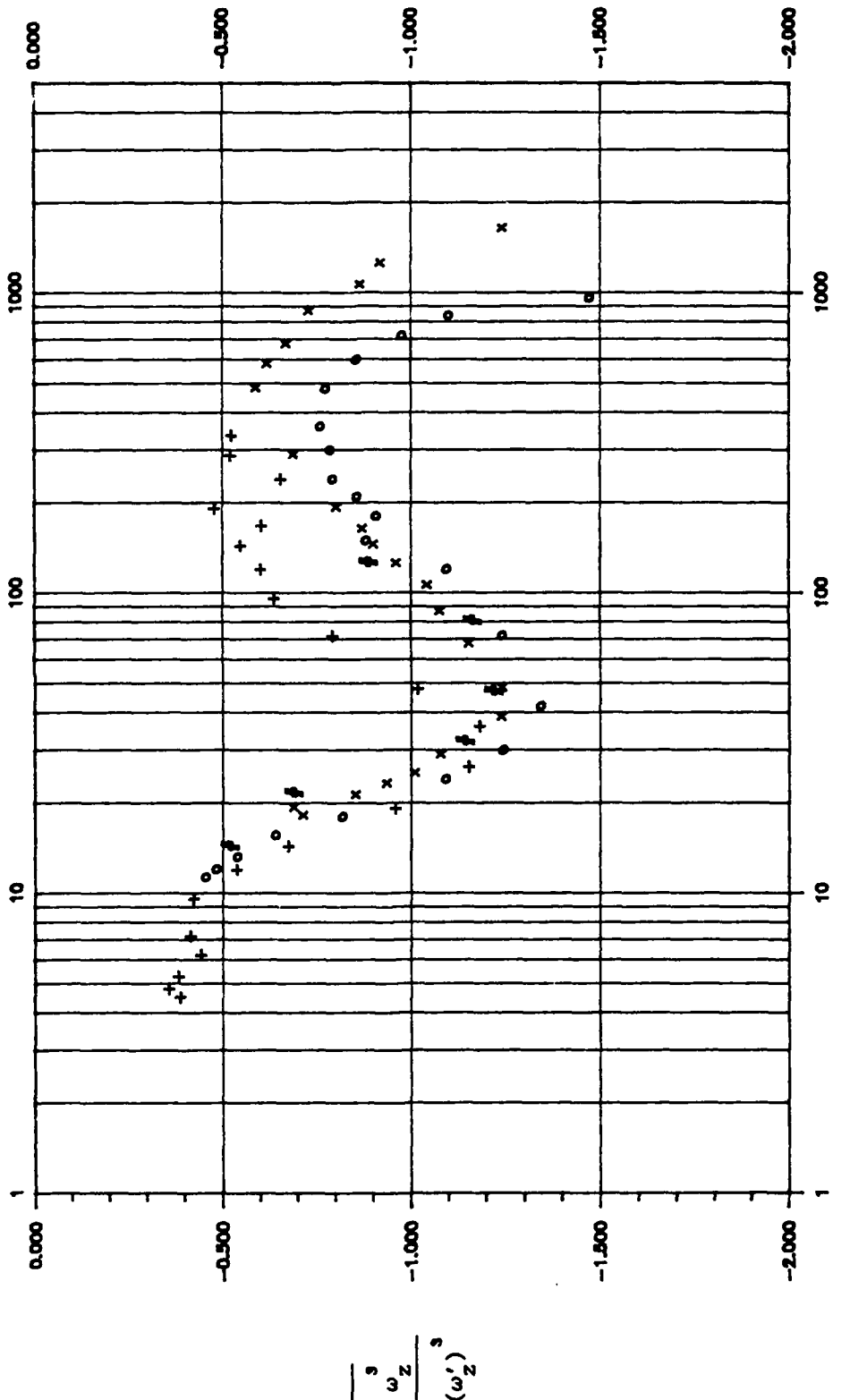

Figure 6. The Skewness of ω_z. # are data of Balint et. al. (1986).

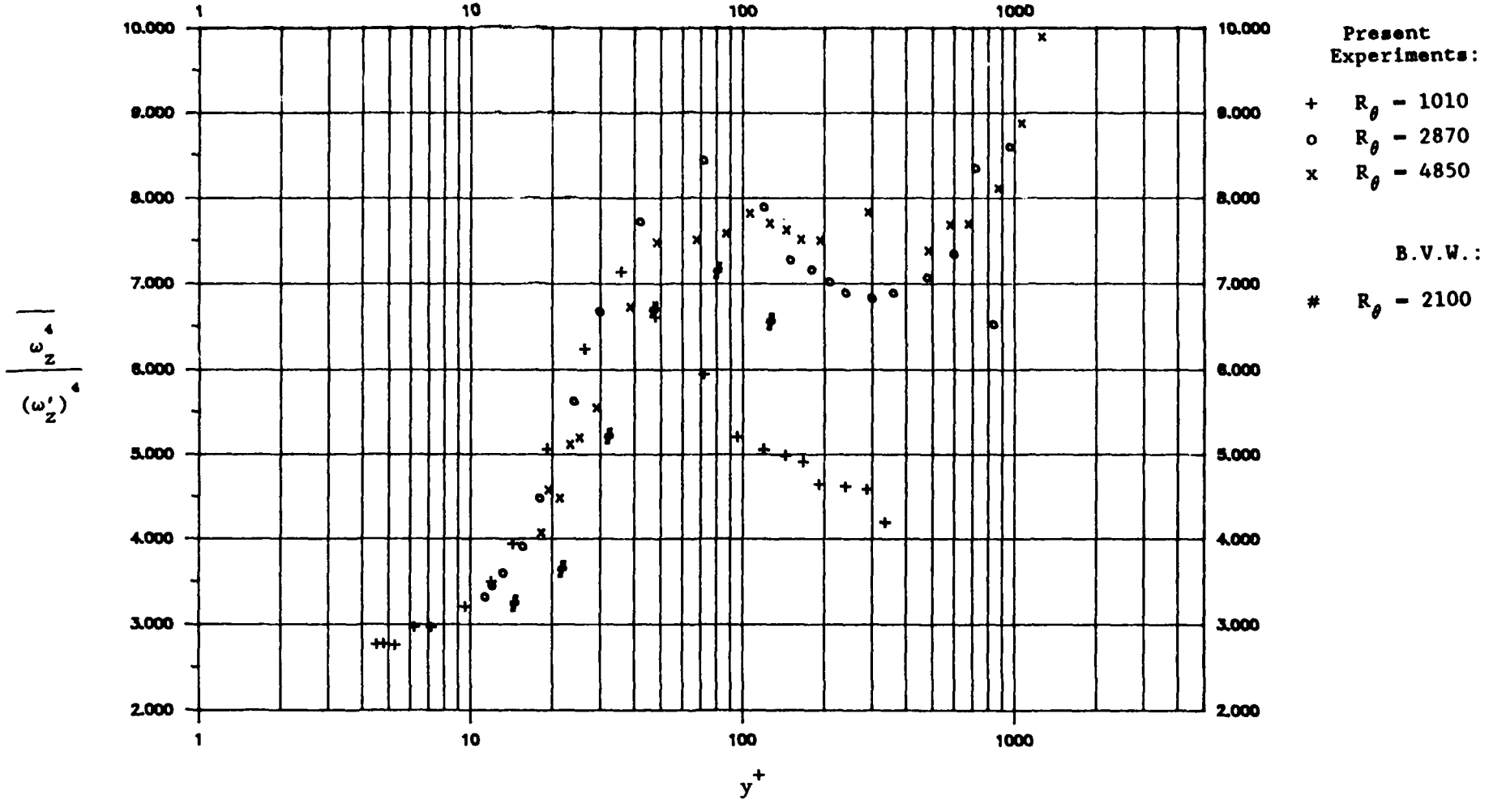

Figure 7. The Flatness of ω_z. # are data of Balint et. al. (1986).

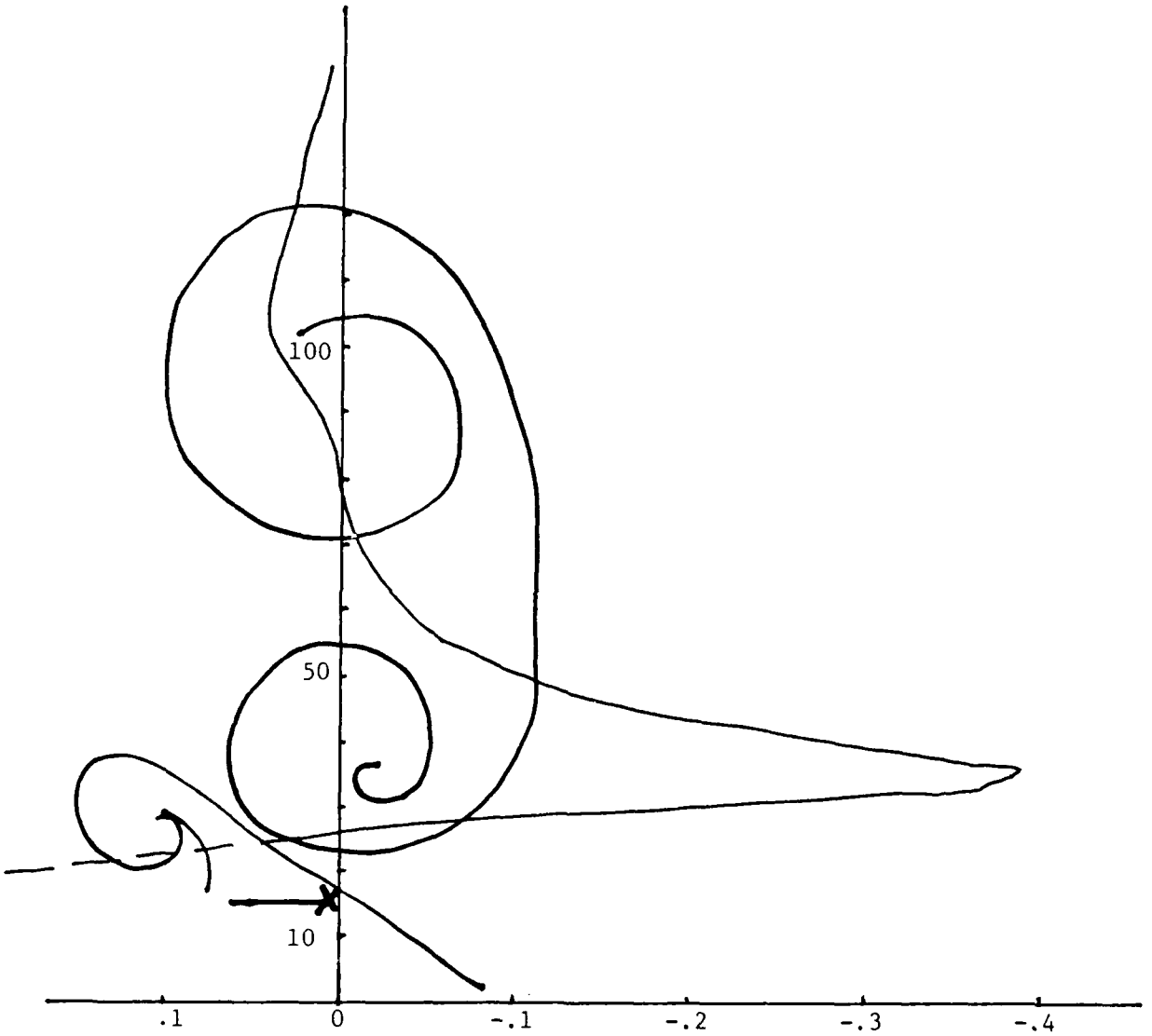

Figure 8. Two-point cross-stream vorticity correlations. Note the strong negative peak of the correlation coefficient at $y^+ = 40$. A Typical eddy and the hairpin it creates has been sketched over the signal (roughly to scale). The event readily explains the strong negative value.

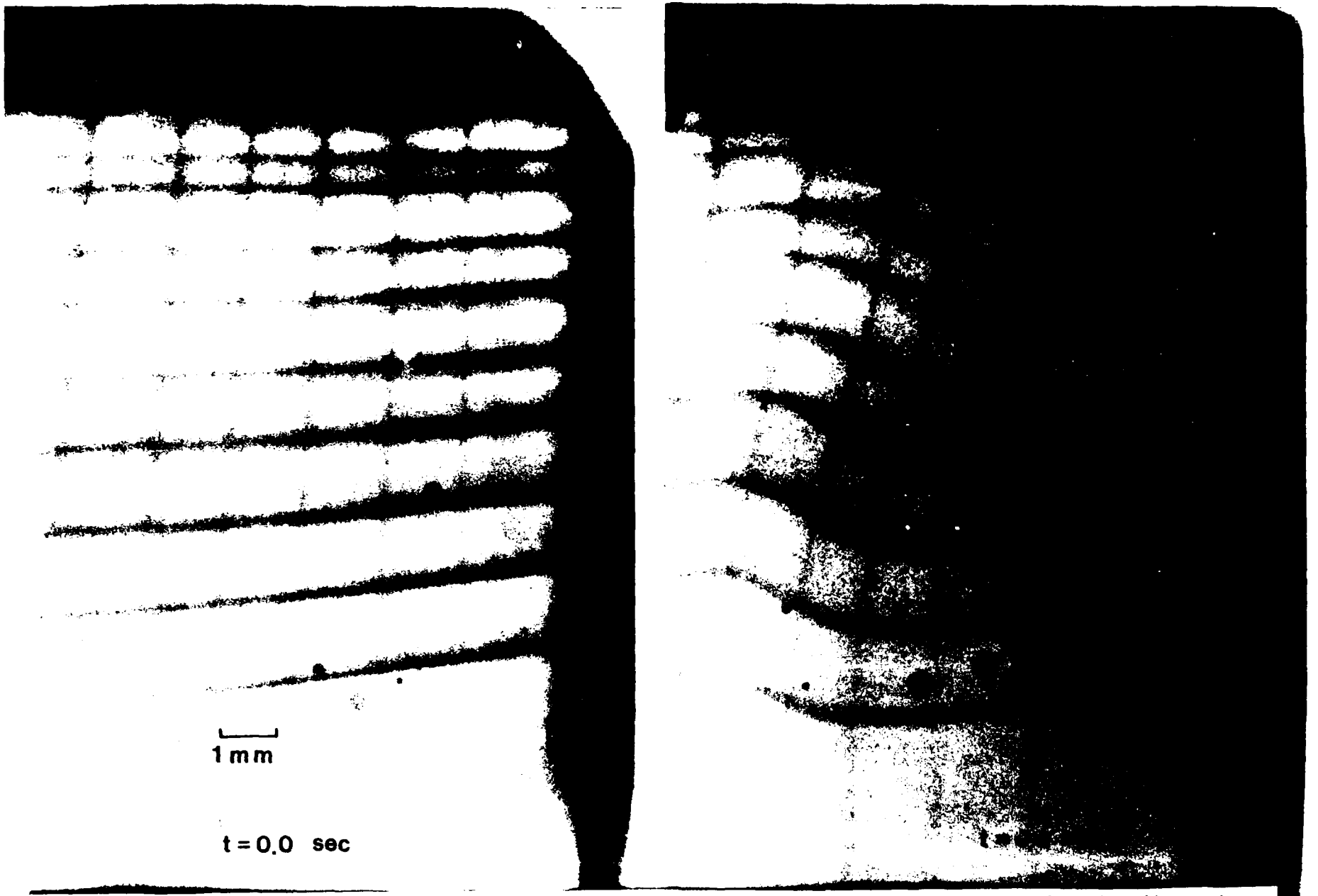

Fig. 9. A Photochromic grid impressed in kerosene. Note the lines are order 100 microns. From its distortion between t = 0 and t = .1 seconds we can measure all of the fluid dynamic quantities in the plane of the picture.

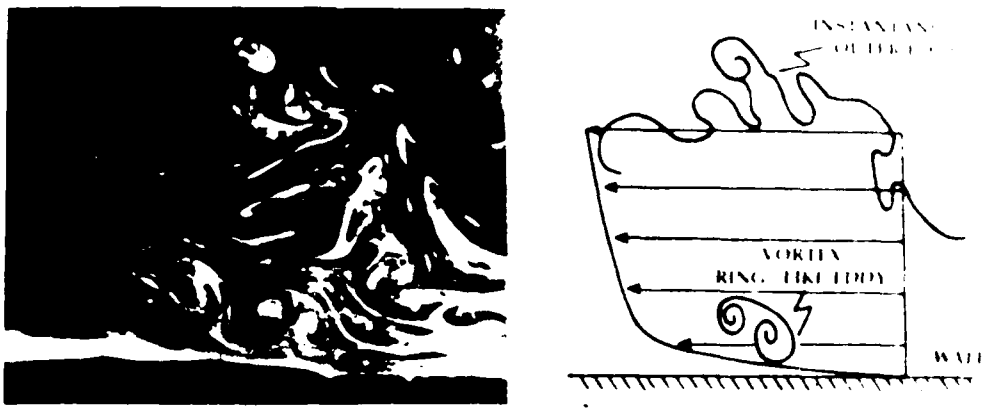

Instantaneous turbulent boundary layer

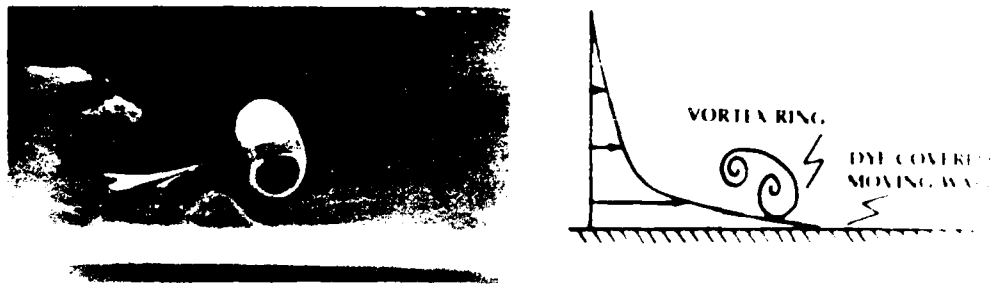

Simulated vortex ring/wall shear layer

Fig. 10. The basic idea behind the simulation. Performing a Galilean transformation on the vortex ring/moving wall interaction makes it a model of the turbulent boundary layer production process.

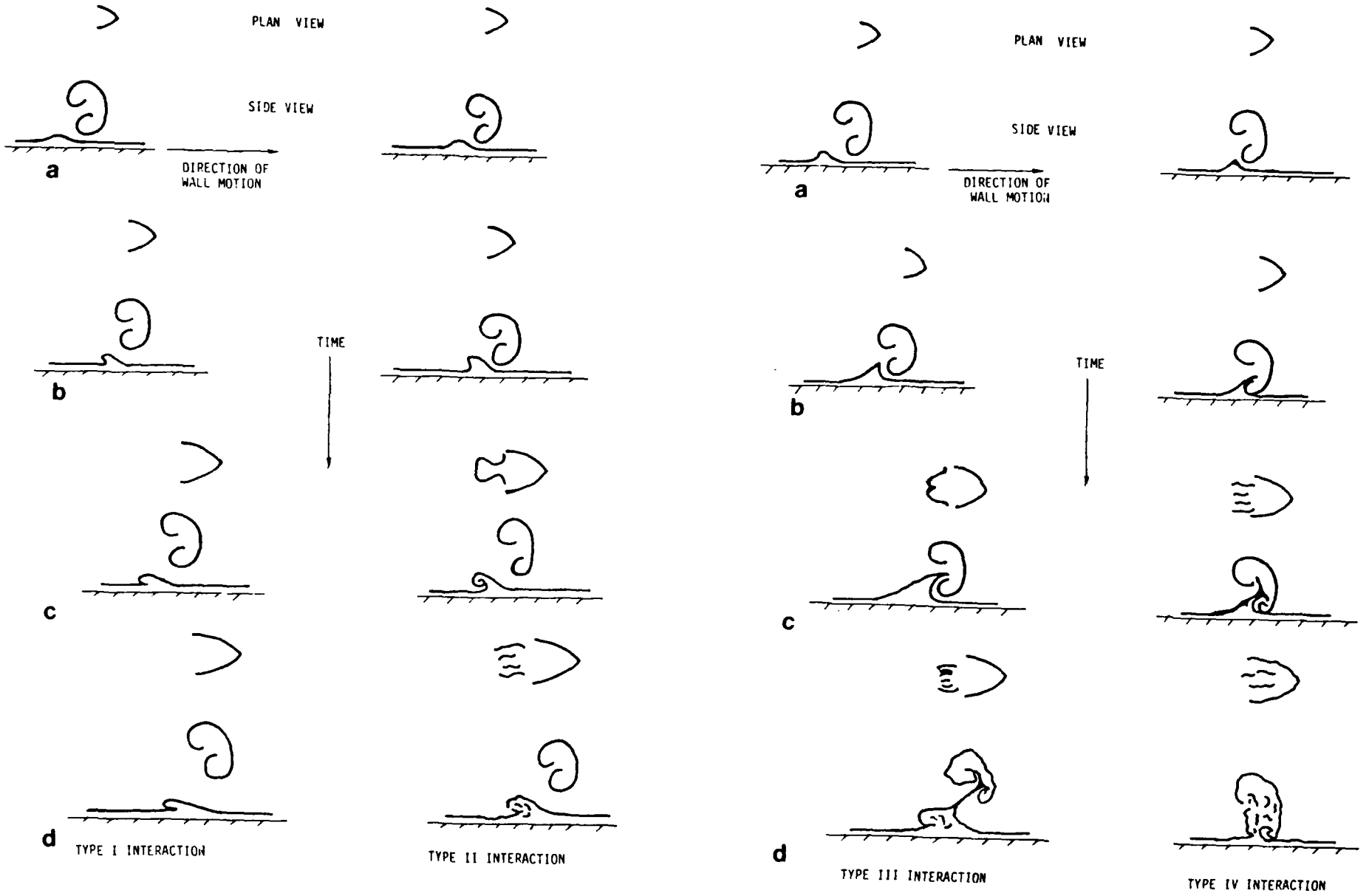

Fig. 11. Sketches of the four types of local vortex ring/moving wall interactions (see text for explanation).

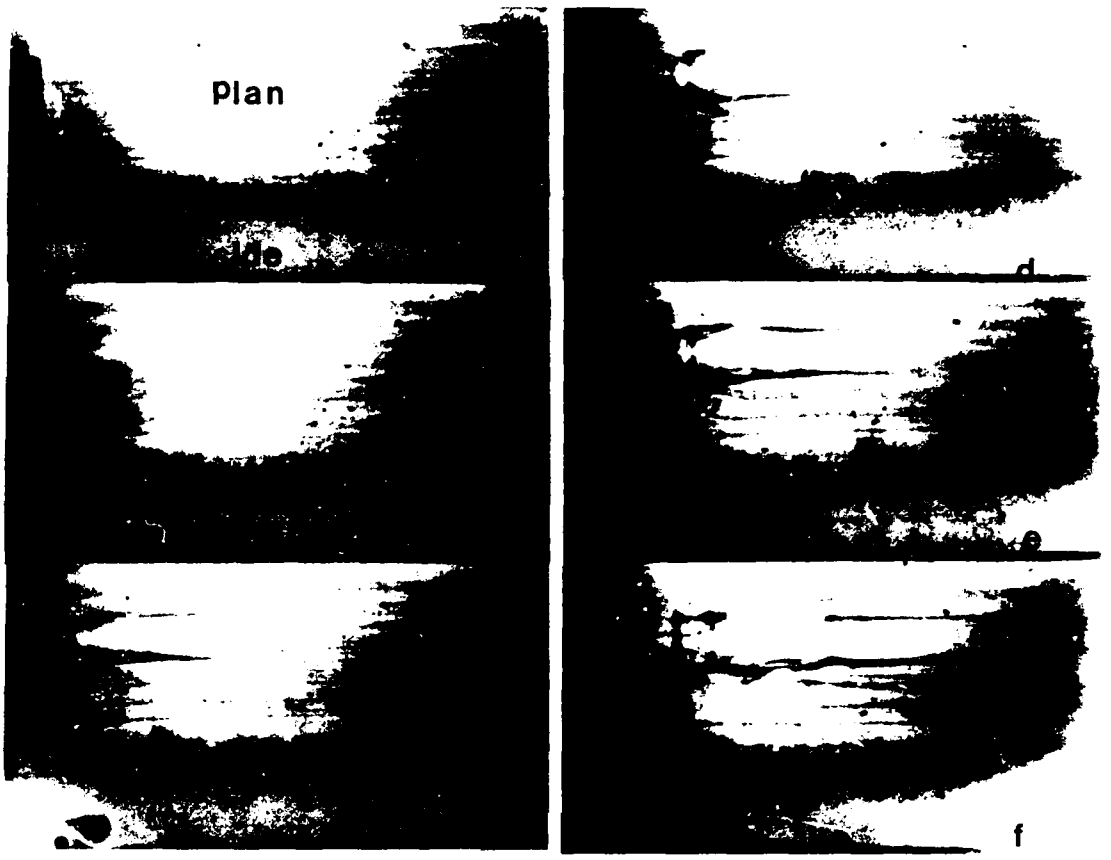

Fig. 12. Six photos of a vortex ring/moving wall interaction for $U_r/U_w \leq .35$ when the ring moves toward the wall at a 3 degree angle. Both plan and side views are shown; the ring and the wall are moving to the right; only the wallward side of the ring has dye in it. The interaction results in a pair of long streaks prior to the onset of a pocket and its associated hairpin lift-up, which then gets partially ingested into the ring.

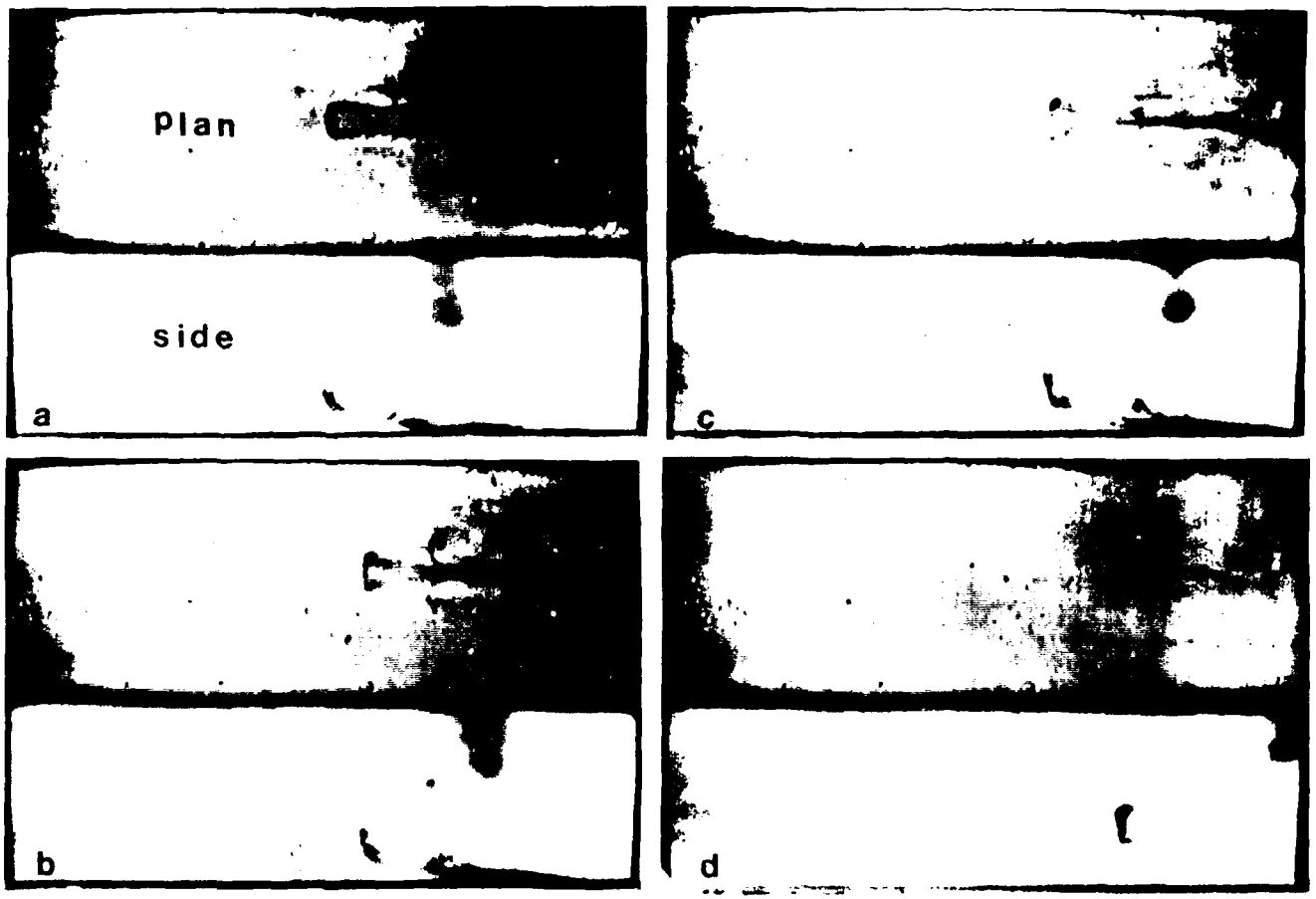

Fig. 13. Four photos of a vortex ring/moving wall interaction for $U_r/U_w > .45$ when the ring is moving away from the wall at a 2.5 degree angle. Both plan and side views are shown; the ring is at the upper right of the side view; ring and wall are moving to the right. A hairpin forms when the interaction starts. The long stable streamwise streaks which also form, come closer and closer together, indicating that the streamwise vorticity which caused them, and which is of opposite sign, is being stretched and coming closer together. This evolution leads to 'pinch-off' and the creation of a new vortex ring.

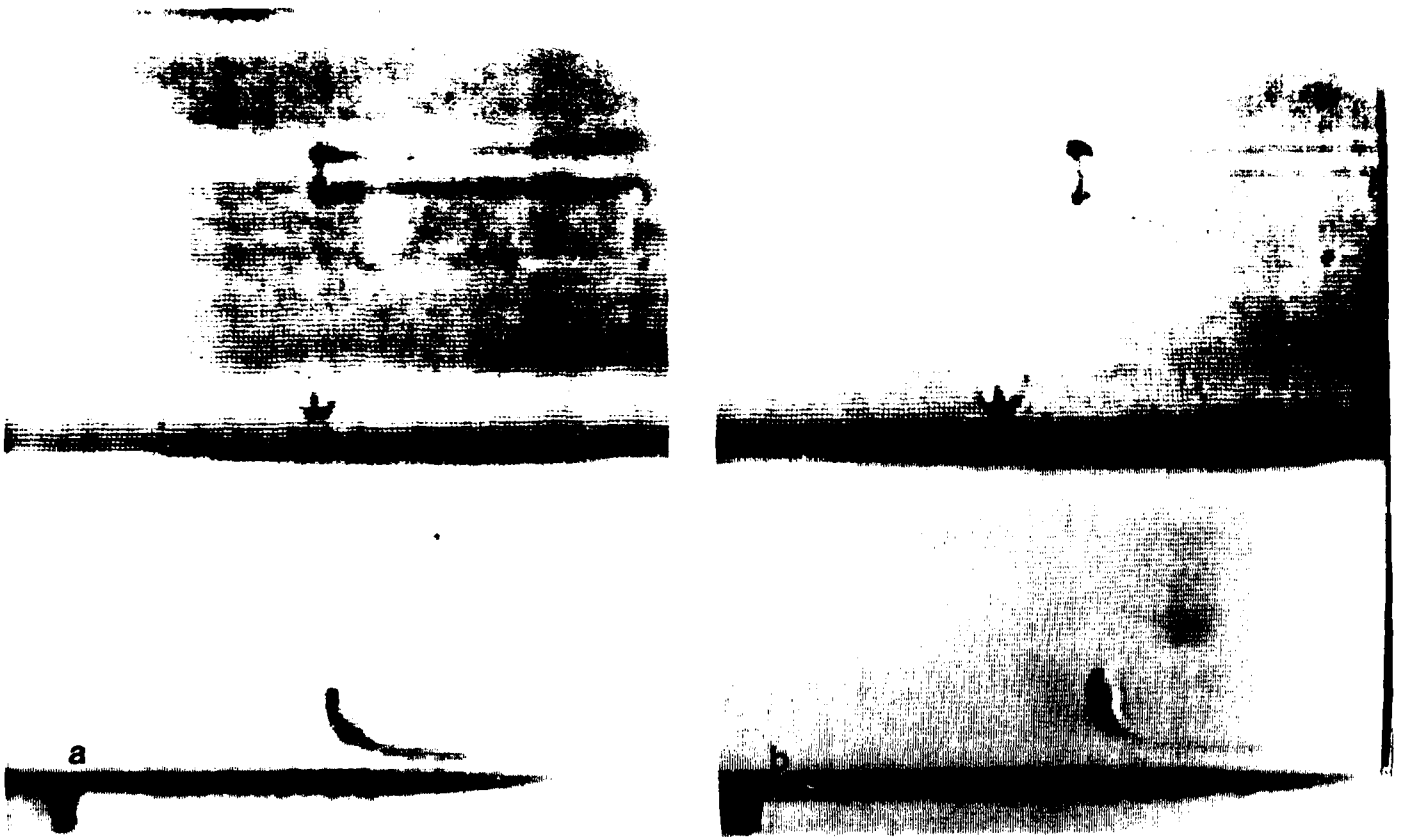

Fig. 14. Same conditions as Fig. 6, except that the wall layer is very thin, so δ/D is small. We obtain long very stable streaks and a long stretched hairpin which does not pinch-off over the 2500 wall layer distance of the facility. The time between each photo is approximately 50 wall units.

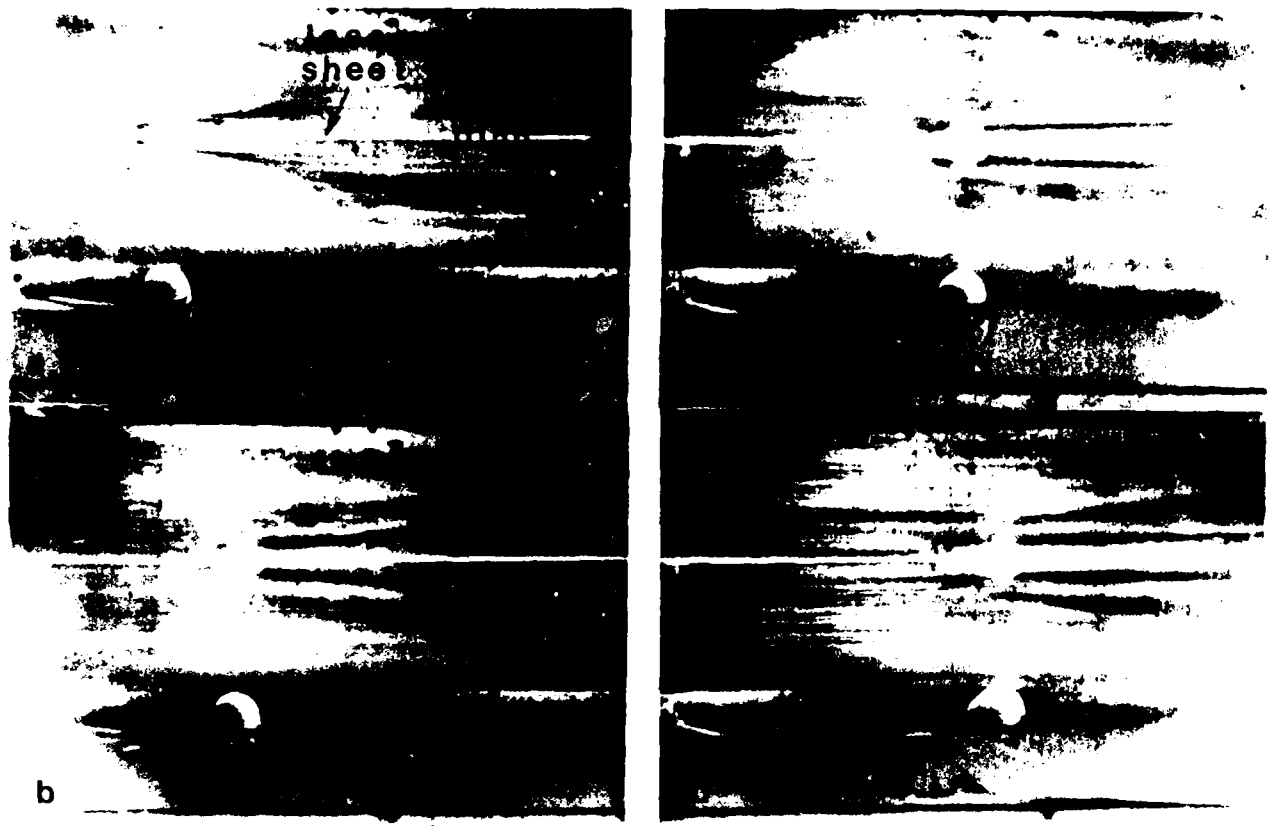

Fig. 15. Four photos of a vortex ring/moving wall interaction for $U_r/U_w < .45$ when the ring is moving away from the wall at a 2.5 degree angle and $\delta/D > .15$. Both plan and side views are shown; the ring has most of its dye in the upper part; ring and wall are moving to the right. Again a pair of long stable streaks is created, a pocket does not form, and a weak hairpin which forms does not pinch-off. There is evidence of a second pair of streaks forming.

AD-A185 560 THE PRODUCTION OF TURBULENCE IN BOUNDARY LAYERS -- THE ROLE OF MICROSCALE..(U) MICHIGAN STATE UNIV EAST LANSING TURBULENCE STRUCTURE LAB R E FALCO JUN 87 2/2

UNCLASSIFIED TSL-87-3 AFOSR-TR-87-1194 F49620-85-C-0002 F/G 20/4 NL

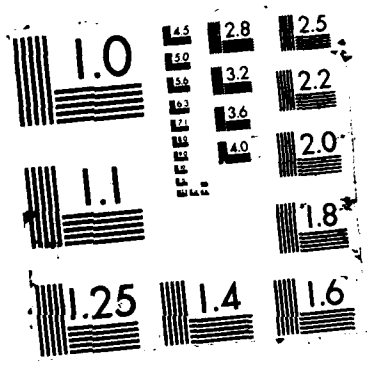
1.0
1.1
1.25
1.4
1.6
2.8
3.2
3.6
4.0
2.5
2.2
2.0
1.8

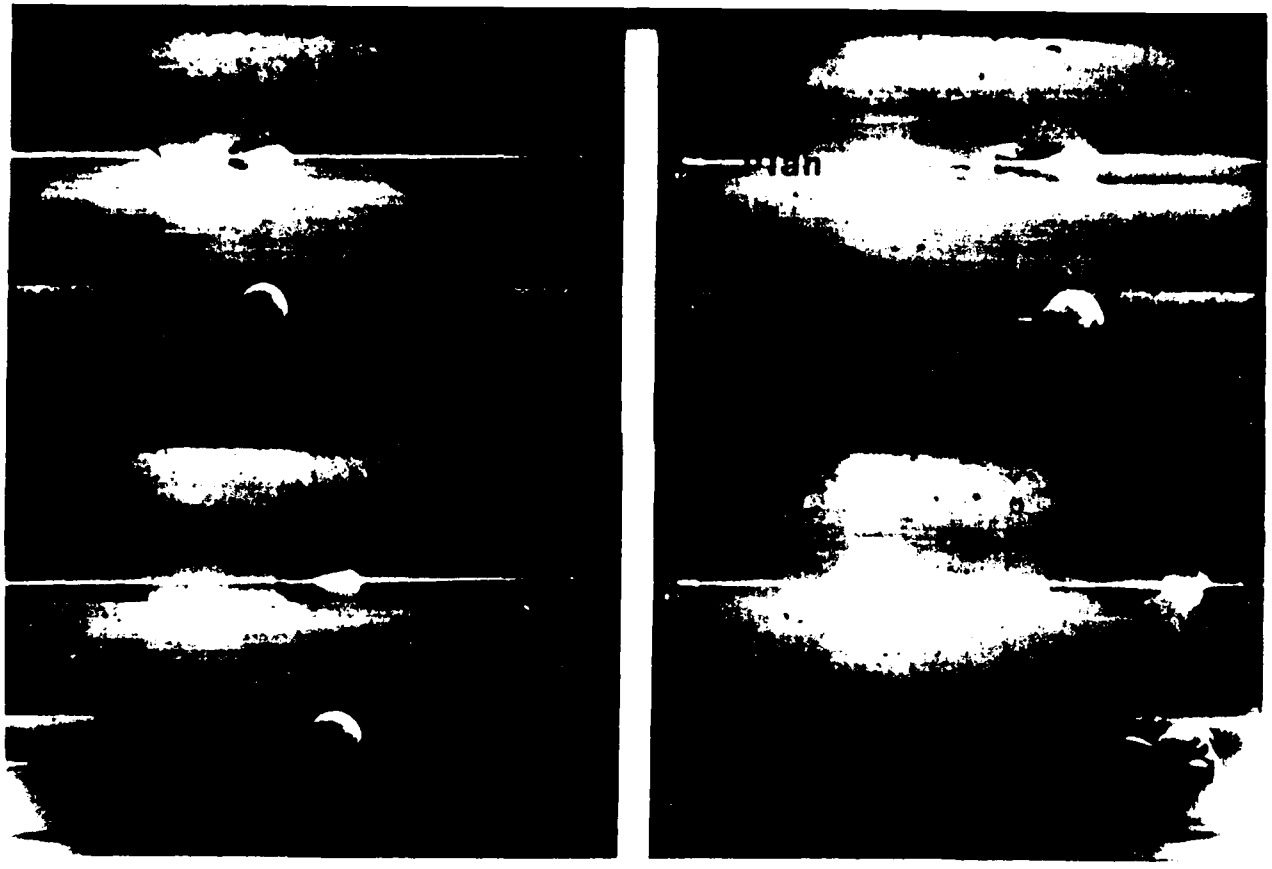

Fig. 16. Same conditions as Fig. 8, except that $\delta/D < .15$. In this case we again obtain a pair of long stable streaks and a hairpin. Pinch-off of a portion of the lifted hairpin does occur creating a new small vortex ring. We don't have the secondary streak pair forming.

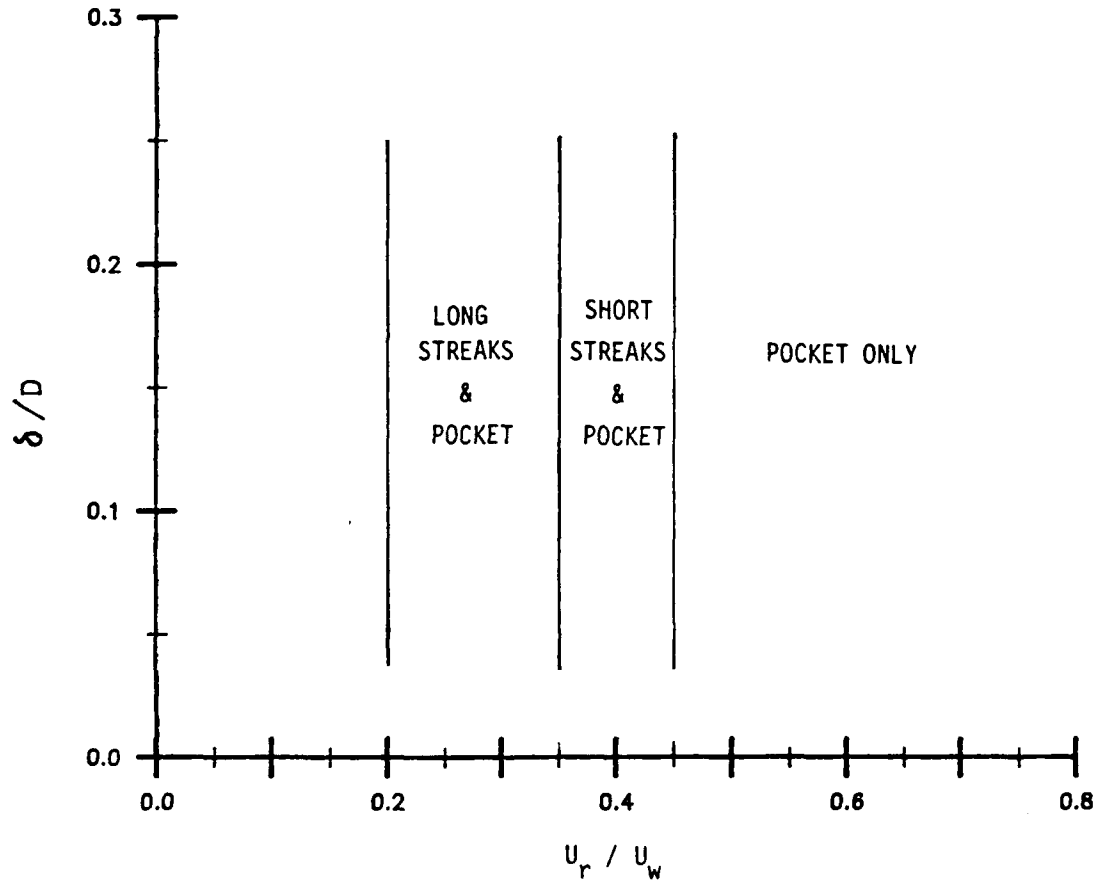

Fig. 17. The dependence of the formation and evolution of streaks on δ/D and U_r/U_w for $D+ > 250$ and a 3 degree incidence angle. The indicated boundaries between different evolutions are approximate. Streaks are only observed to form for $U_r/U_w < .45$.

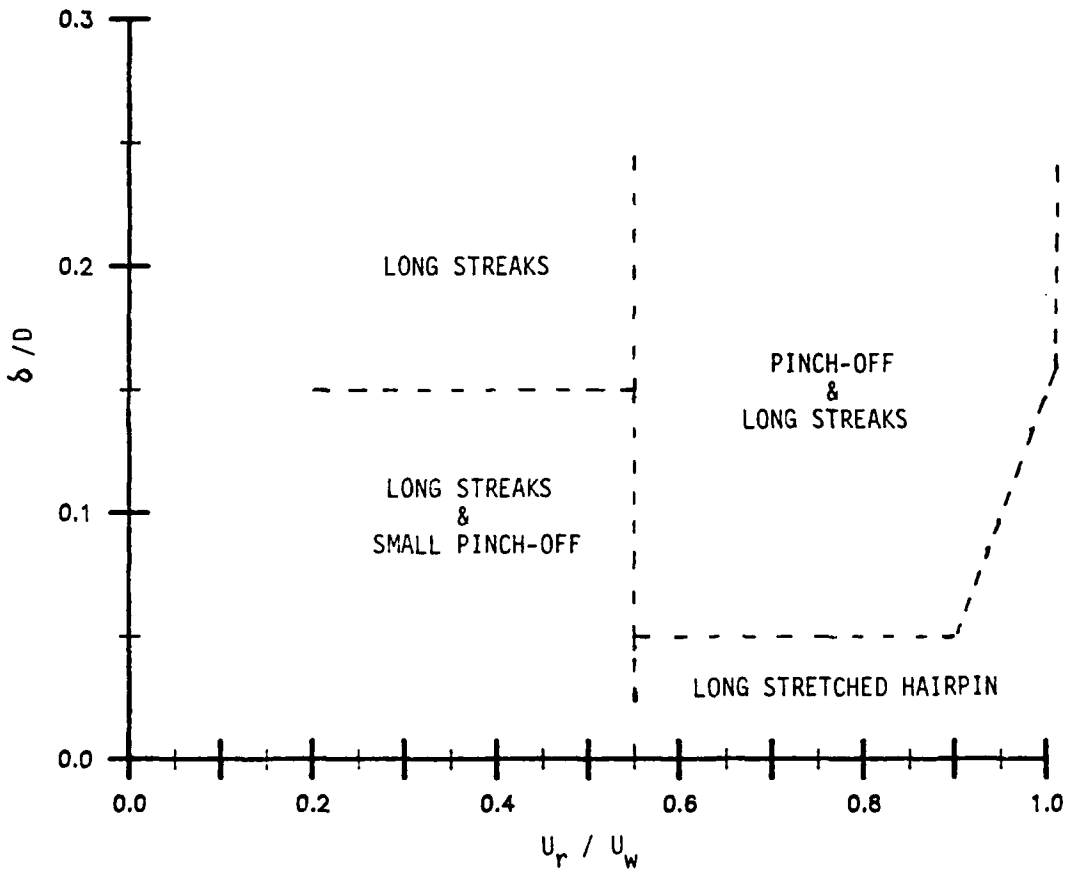

Fig. 18. The dependence of the formation and evolution of streaks on δ/D and U_r/U_w for rings moving away from the wall at 2.5 degrees. δ/D now plays a much important role, and long streaks are generated over the entire speed ratio range studied.

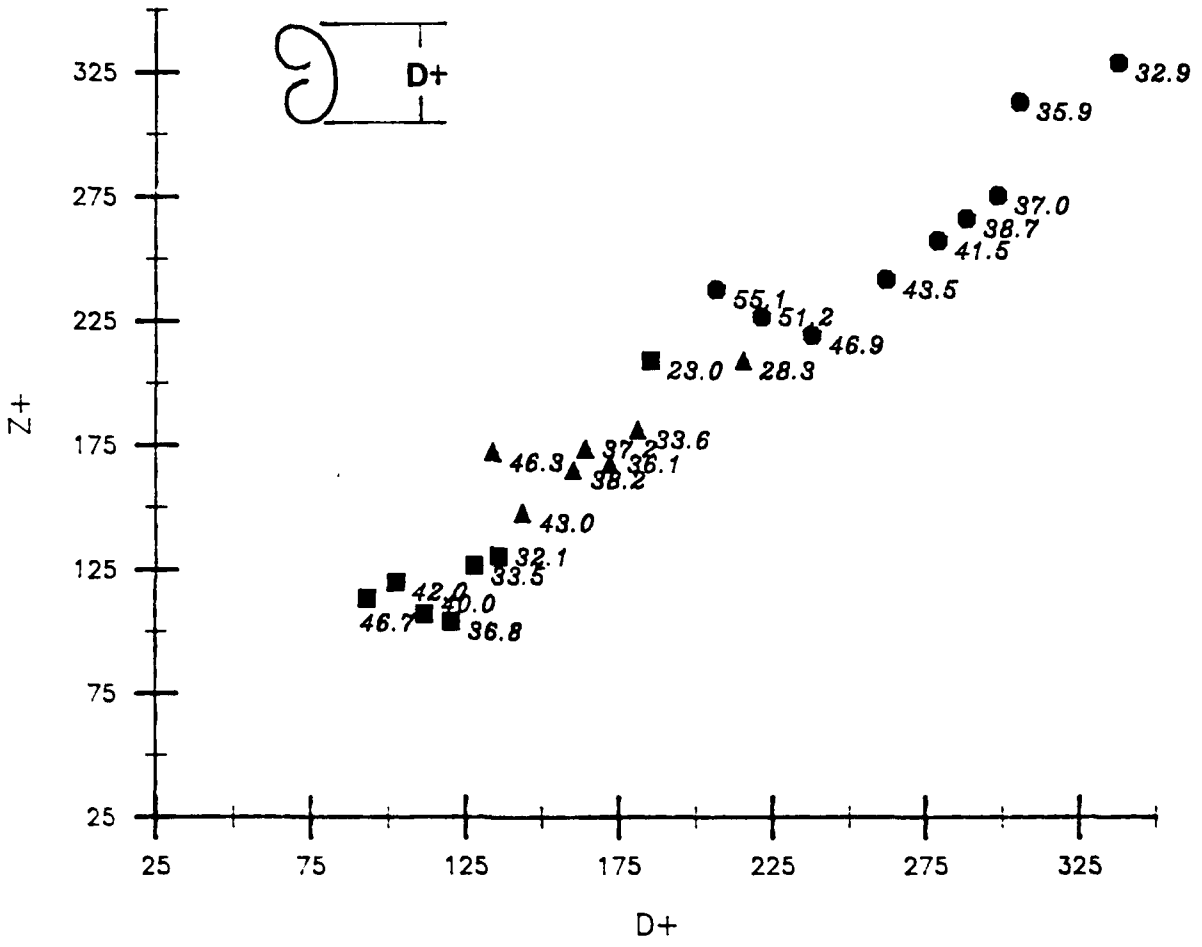

Fig. 19. The dependence of the long streak spacing in wall units on the size of the vortex ring in wall units, for an incidence angle of 3 degrees and U_r/U_w = .31. The thickness of the wall layer (in wall units) is shown next to each data point.

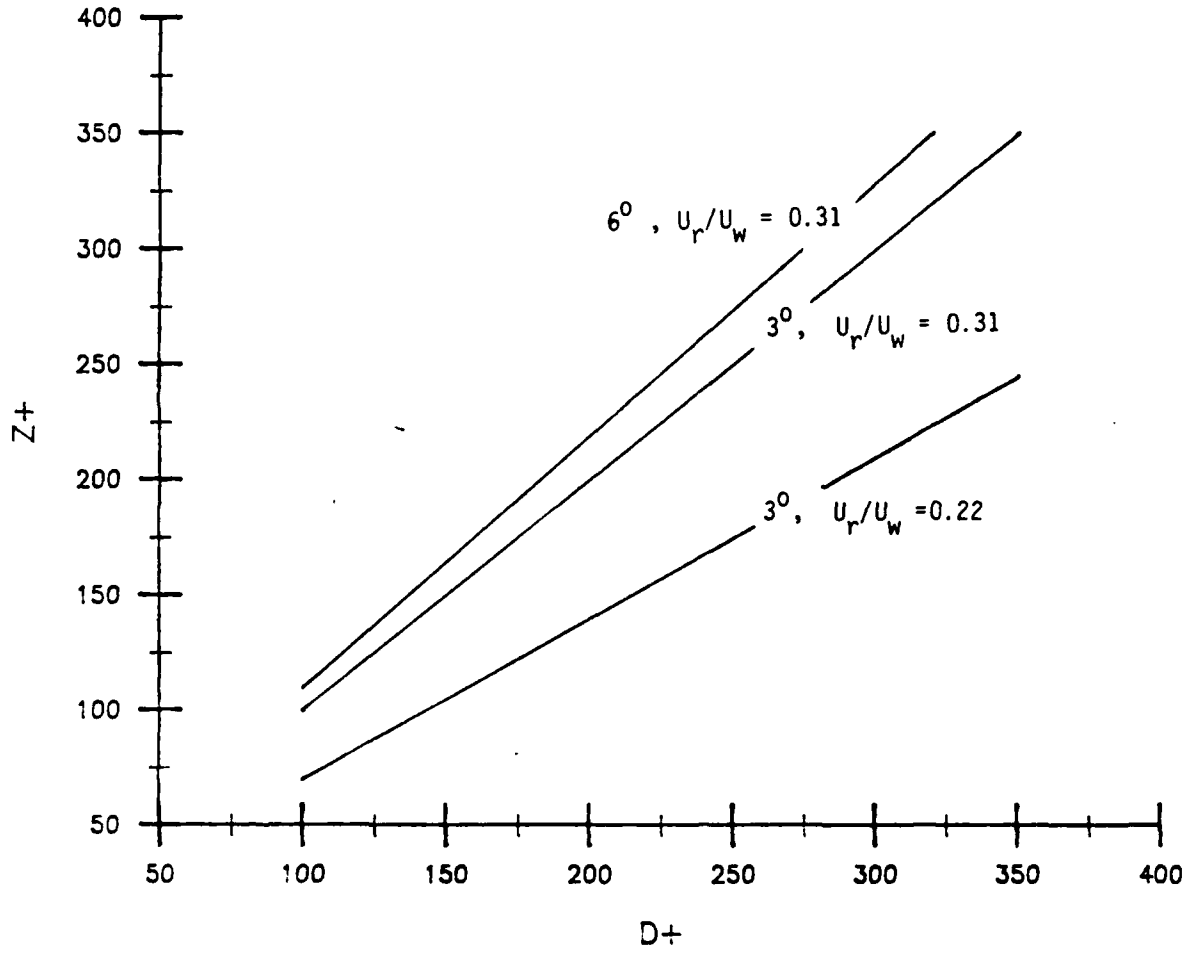

Fig. 20. The dependence of the streak spacing on the speed ratio and ring interaction angle.

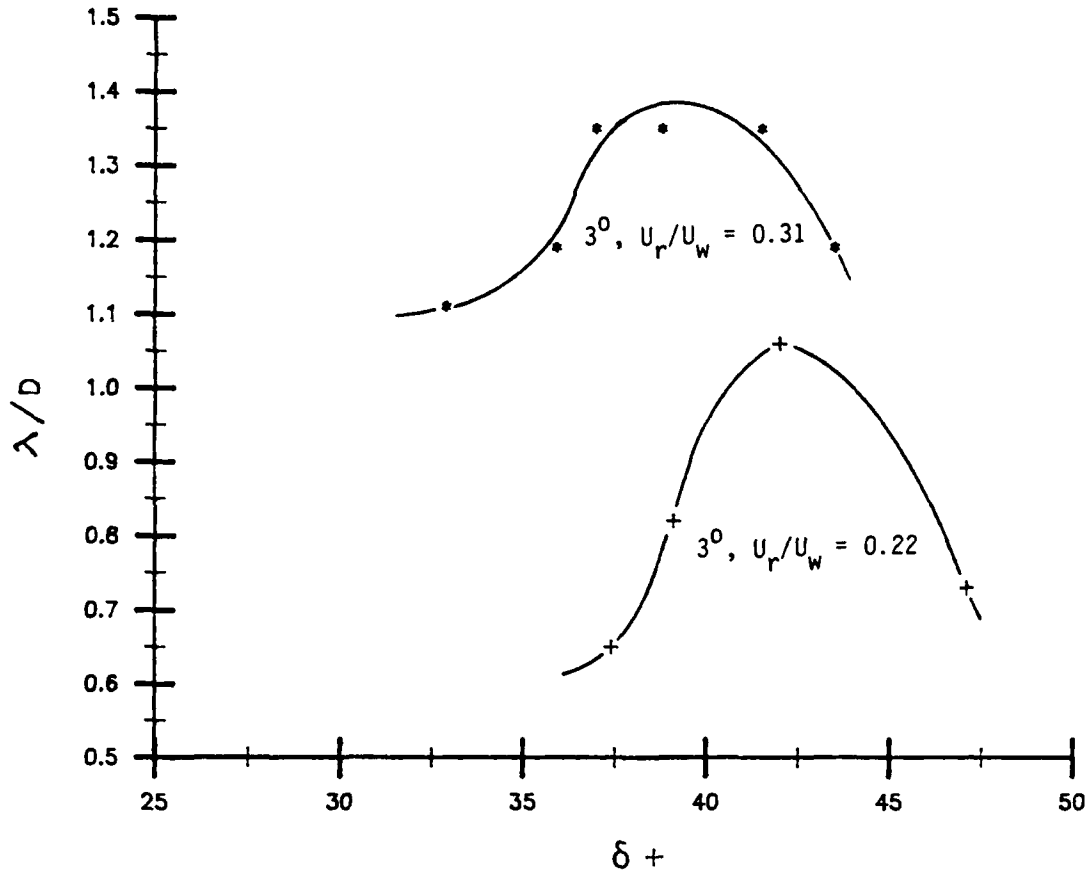

Fig. 21. The non-dimensionalized streamwise wavelength of streaks subjected to wavy instabilities.

STABILITY BOUNDARIES

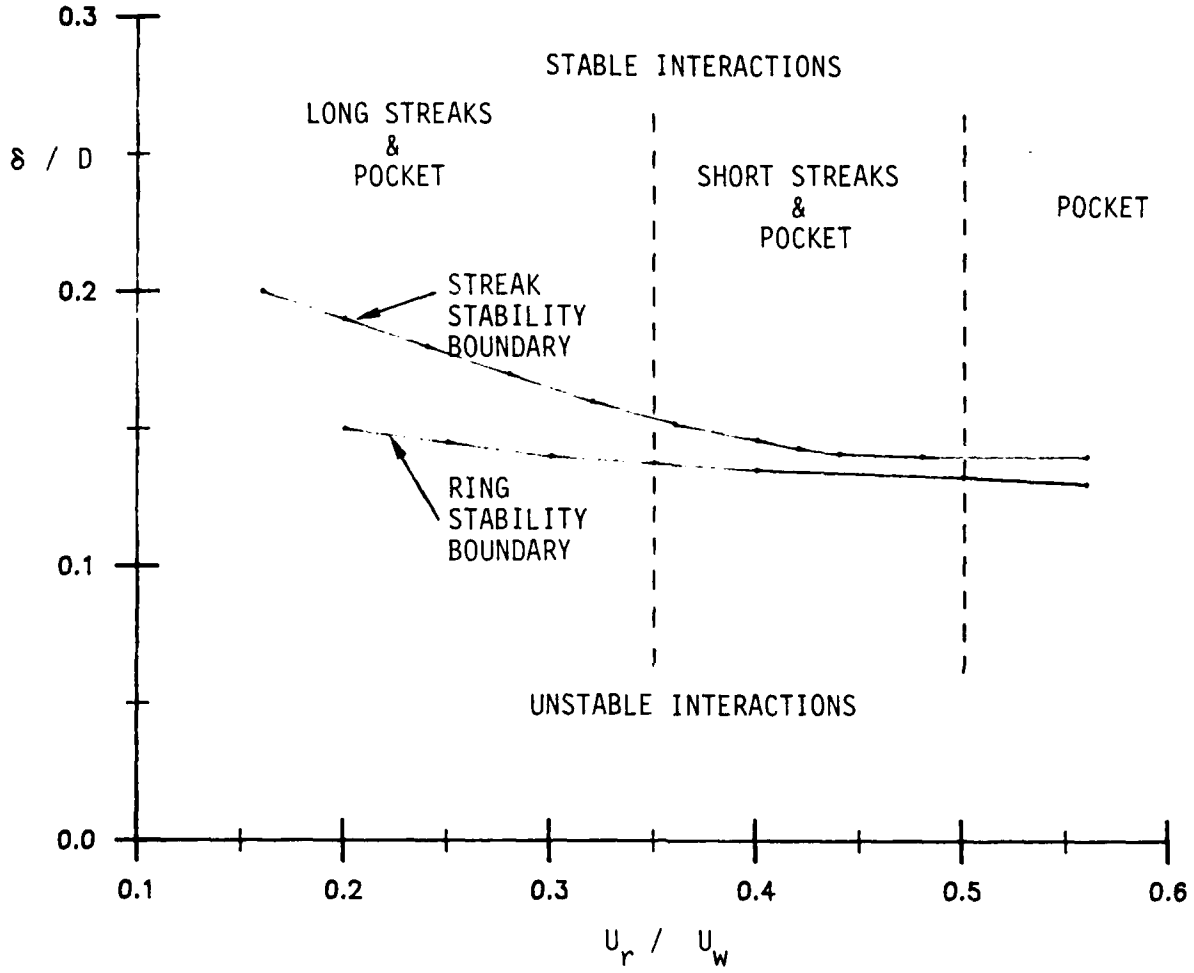

Fig. 22. Comparison of the 'stability boundaries' of a three degree ring moving towards the wall, and of the boundaries of stable streak formation those rings can create. The ring stability curves and the streak stability boundary curves for different size rings collapse when plotted this way.

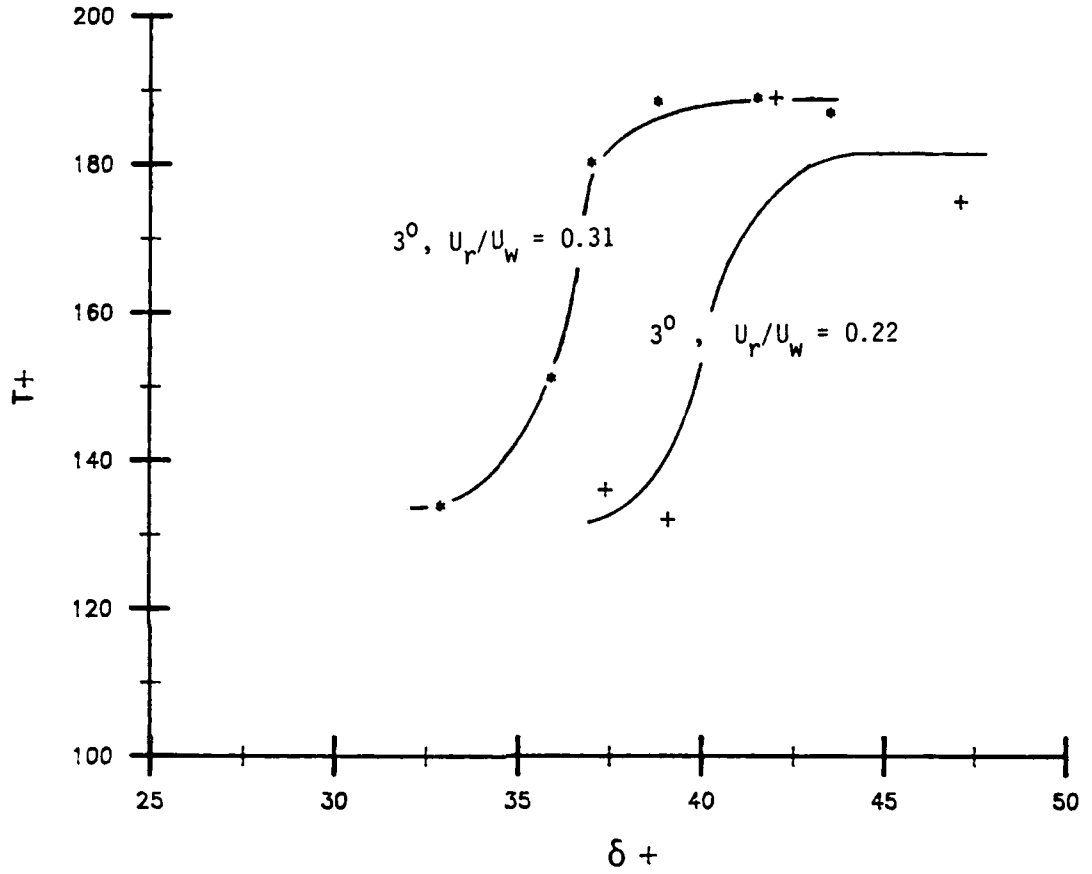

Fig. 23. The dependence of the time to instability of the streaks on the wall layer thickness (both quantities non-dimensionalized by wall layer variables) for 3 degree incidence rings.

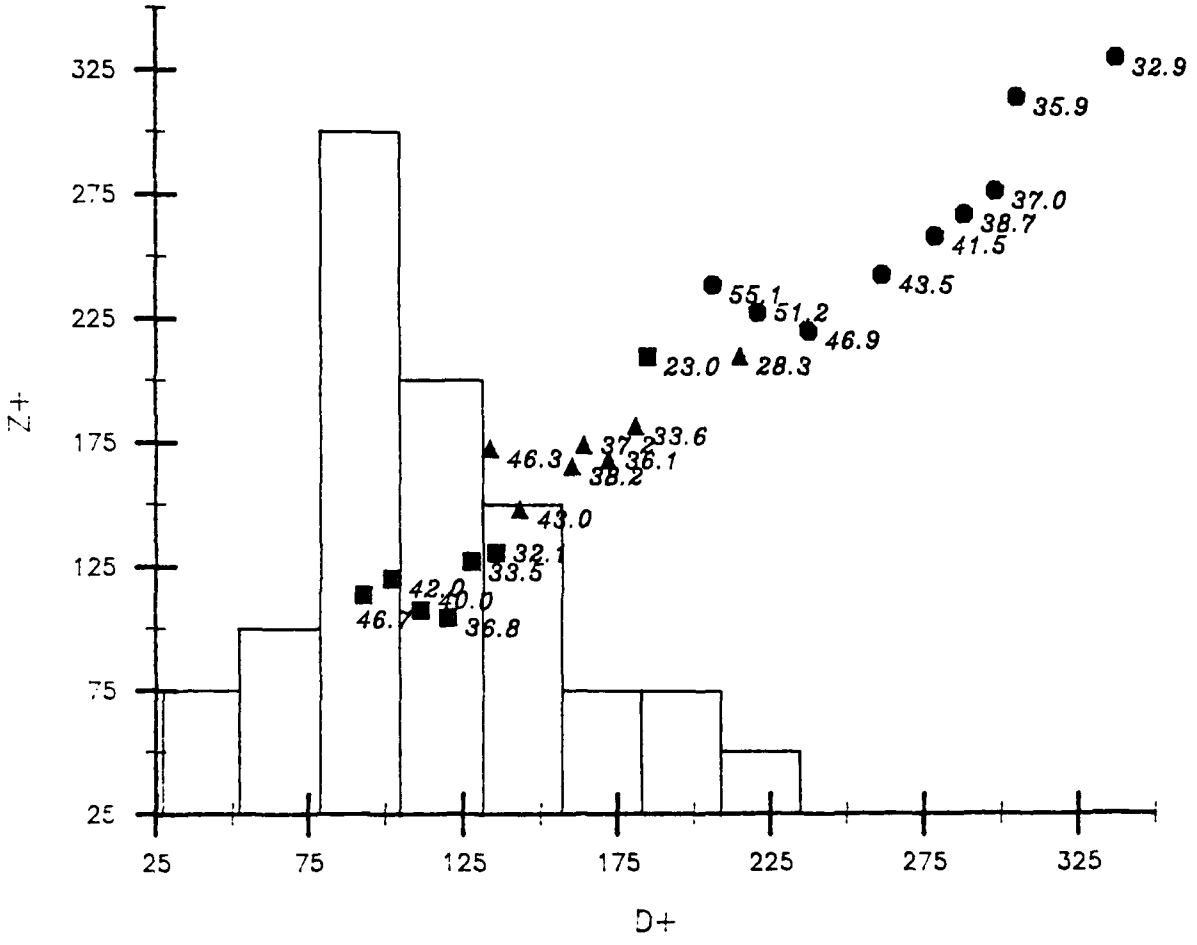

Fig. 24. The distribution of D^+ obtained from the diameter of the Typical eddies of a turbulent boundary layer at R = 1176, superimposed upon the streak spacing obtained for various size rings.

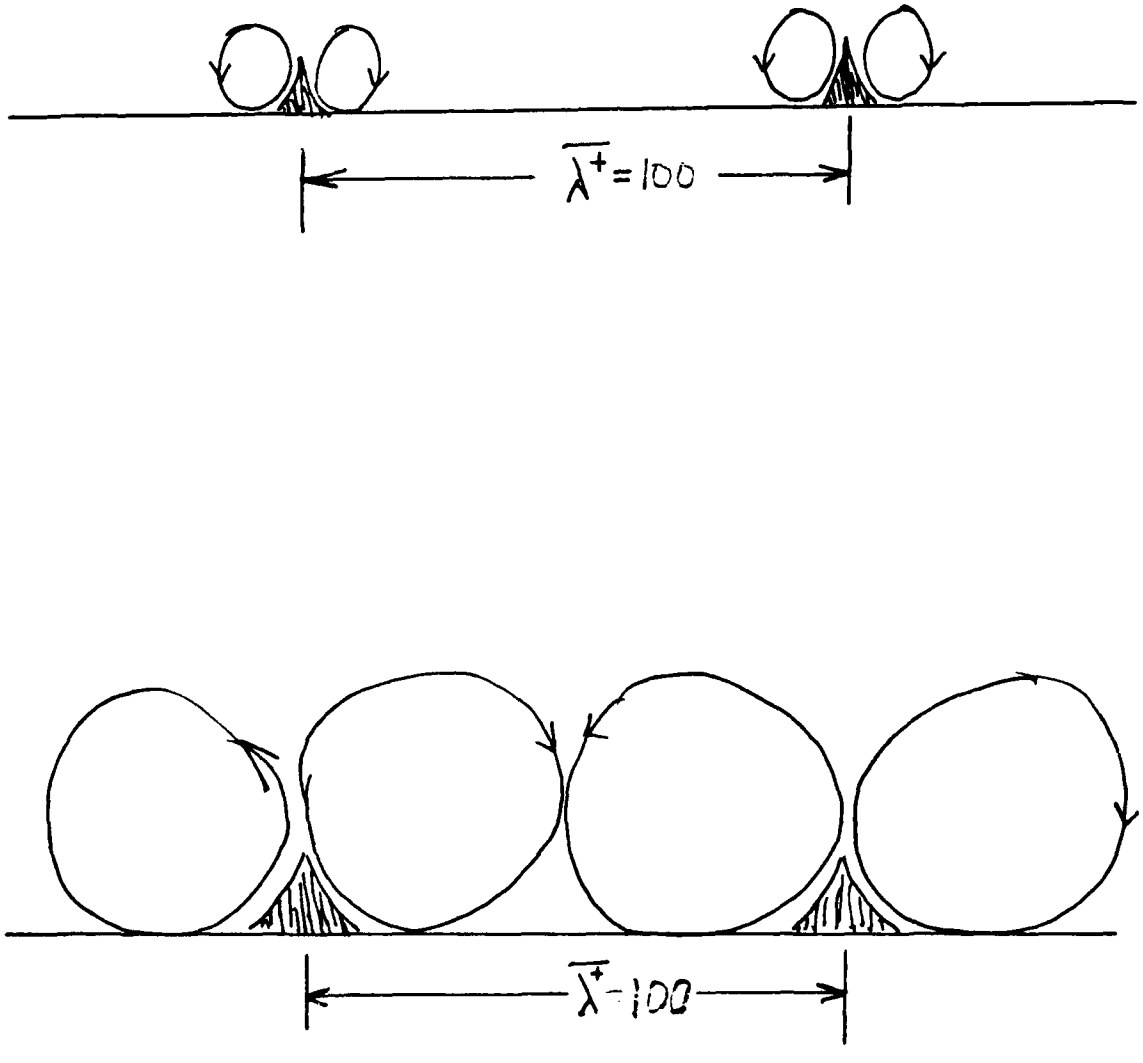

Figure 25. a) Vortex pairs observed to be associated with lifting low speed streaks. b) The familar sketch of the process hypothesized by many investigators.

END

12-87

DTIC